

Supporting Information

Ultrasonic exfoliation of a Cd-based metal–organic framework into ultrathin nanosheet for visible-light-initiated trifluoromethylation and sequential oxidation–cyclisation reaction

Xiong-Feng Ma,^a Jianfei Tong,^a Zhuang Miao,^a Xiaodun Deng,^a Zhiqiang Zhang,^a Chunyang Zhao,^{*,c} Yangyang Liu,^a Chengyu Xi,^a Hongliang Du,^{*,a} Chaoqian Ai,^a Wenke Li,^a Hui Chen,^{*,b}

^a *College of Engineering, Xi'an International University, Xi'an, Shaanxi, China.*

^b *School of Chemistry and Chemical Engineering, Xi'an University of Architecture and Technology, Xi'an, Shaanxi, China.*

^c *School of Science, Xihua University, Chengdu, Sichuan, China*

*Correspondence Email: duhongliang@126.com, huichen@xauat.edu.cn, 0120240049@xhu.edu.cn

Experimental Section

Materials and Measurements.

All reagents and solvents are commercially available (Beijing innoChem Science & Technology Co. Ltd.), and they were further dried by the vacuum rotary evaporator to remove all traces of water and then stored in the air-filled glovebox. The 15 mL Schlenk tube charged with a magnetic stirrer, which was used as the reactor in the thioether oxidation and benzyl alcohol dehydrogenation reactions. The light was provided by a 30 W red LED light.

The chemical structures of the products were confirmed by comparison with standard chemicals and GC-MS (Agilent Technologies, GC 7890B, MS 5977A) data. GC equipped with a FID detector (Agilent Technologies, GC 7890 B) and a HP-5 5% phenyl methyl siloxane column (30m × 0.32mm × 0.5 μm), which was used for the quantifiable measure of benzotrifluoride and 2-phenylbenzimidazole. The size and morphology of catalysts were measured by a Hitachi New Generation SU8010 field emission scanning electron microscope (FE-SEM, JSM-670 F). The transmission electron microscopy (TEM) images, high-resolution transmission electron microscopy (HRTEM) images (with an acceleration voltage of 200 kV), and selected area fast Fourier transform (FFT) pattern were measured on a JEOL JEM-3000F microscope, which with a CCD camera as the detector. A Varian Cary 500 UV-Vis spectrophotometer was used to record the UV-Vis diffuse reflectance spectra (DRS) of various solid samples. The photoelectrochemical characterization was performed on a Metrohm-Autolab AUT302N Electrochemical workstation. Photocurrent measurements were carried out in a typical three-electrode configuration with an Ag/AgCl electrode, a coiled Pt wire as the reference and counter electrode, respectively. X-ray diffraction (XRD) studies of catalyst were carried out with a Bruker D8 Advance instrument. The electron paramagnetic resonance (EPR) experiments were carried out on Bruker A300 instrument operating in the X-band at room temperature.

Single-crystal X-ray crystallography.

Diffraction data for all complexes were measured on a Bruker SMART CCD diffractometer (Mo K α radiation and $\lambda = 0.71073 \text{ \AA}$) in Φ and ω scan modes. All structures were solved by direct methods, followed by difference Fourier syntheses, and then refined by full-matrix least-squares techniques on F^2 using SHELXL.^[1] All other non-hydrogen atoms were refined with anisotropic thermal parameters. Hydrogen atoms were placed in the calculated position and refined in the isotropic direction using a riding model. Table S1 summarizes X-ray crystallographic data and refinement details for the complexes. The CCDC reference number is 2494196 for **XAIU-5**.

[1] Sheldrick, G. M. *Acta Crystallogr., Sect. C: Struct. Chem.* **2015**, *71*, 3-8.

Table S1. Crystallographic data of **XAIU-5**.

Complex	XAIU-5
Formula	C ₂₀ H ₁₈ CdNO ₆
Formula weight	480.75
<i>T</i> (K)	100.00 (10)
Crystal system	Triclinic
Space group	<i>P</i> -1
<i>a</i> (Å)	9.0623 (2)
<i>b</i> (Å)	10.2537 (2)
<i>c</i> (Å)	13.1574 (2)
<i>α</i> (°)	103.975 (2)
<i>β</i> (°)	94.456 (2)
<i>γ</i> (°)	90.700 (2)
<i>V</i> (Å ³)	1182.23 (4)
<i>Z</i>	2
<i>D_c</i> (g cm ⁻³)	1.351
<i>μ</i> (mm ⁻¹)	7.665
Reflns coll.	13486
Unique reflns	4670
<i>R</i> _{int}	0.0322
^a <i>R</i> ₁ [<i>I</i> ≥ 2σ(<i>I</i>)]	0.0440
^b <i>wR</i> ₂ (all data)	0.1513
GOF	1.175

$${}^aR_1 = \frac{\sum ||F_o| - |F_c||}{\sum |F_o|}, {}^b wR_2 = \left[\frac{\sum w(F_o^2 - F_c^2)^2}{\sum w(F_o^2)^2} \right]^{1/2}$$

Table S2. Selected bond lengths (Å) and angles (°) of **XAIU-5**.

Bond lengths (Å)					
Cd1—O2 ⁱ	2.307 (4)	Cd1—O4 ⁱⁱ	2.345 (4)	Cd1—O5	2.257 (4)
Cd1—O3 ⁱⁱ	2.399 (4)	Cd1—O1	2.232 (4)	Cd1—O6	2.345 (5)
Bond angles (°)					
O2 ⁱ —Cd1—O3 ⁱⁱ	93.80 (13)	O5—Cd1—O4 ⁱⁱ	145.94 (14)	O1—Cd1—O3 ⁱⁱ	141.99 (13)
O2 ⁱ —Cd1—O4 ⁱⁱ	100.87 (14)	O5—Cd1—O6	85.21 (18)	O1—Cd1—O5	126.61 (14)
O2 ⁱ —Cd1—O6	165.81 (18)	O4 ⁱⁱ —Cd1—O3 ⁱⁱ	55.42 (12)	O1—Cd1—O4 ⁱⁱ	86.91 (13)
O5—Cd1—O2 ⁱ	81.62 (14)	O4 ⁱⁱ —Cd1—O6	92.99 (19)	O1—Cd1—O6	84.92 (17)
O5—Cd1—O3 ⁱⁱ	90.58 (13)	O1—Cd1—O2 ⁱ	98.72 (14)	O6—Cd1—O3 ⁱⁱ	91.58 (17)
Symmetry codes: (i) -x+1, -y+1, -z+1; (ii) x, y-1, z; (iii) -x+2, -y+2, -z+2; (iv) x, y+1, z.					

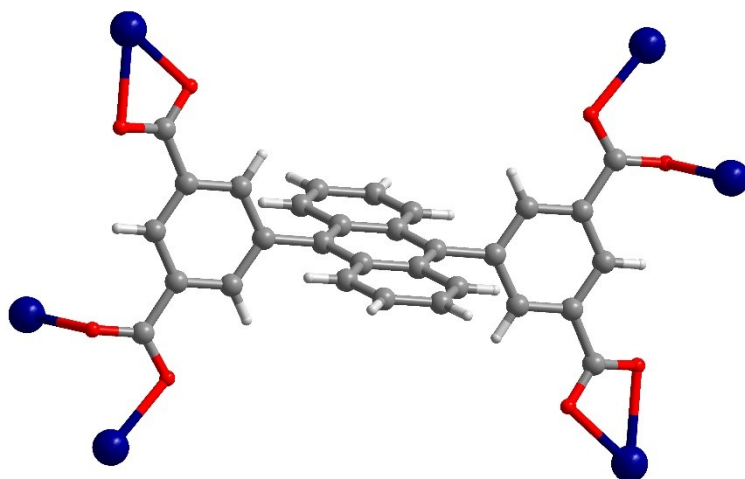


Figure S1. The coordinated mode for ADPA⁴⁻ ligand for XAIU-5.

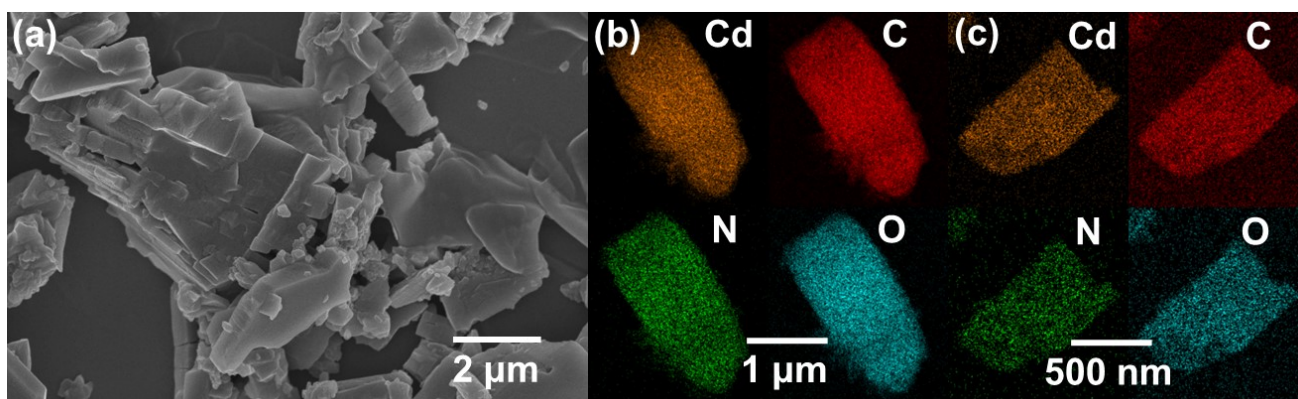


Figure S2. (a) The FE-SEM images of XAIU-5; TEM mapping images of XAIU-5 (b) and XAIU-5-NS (c).

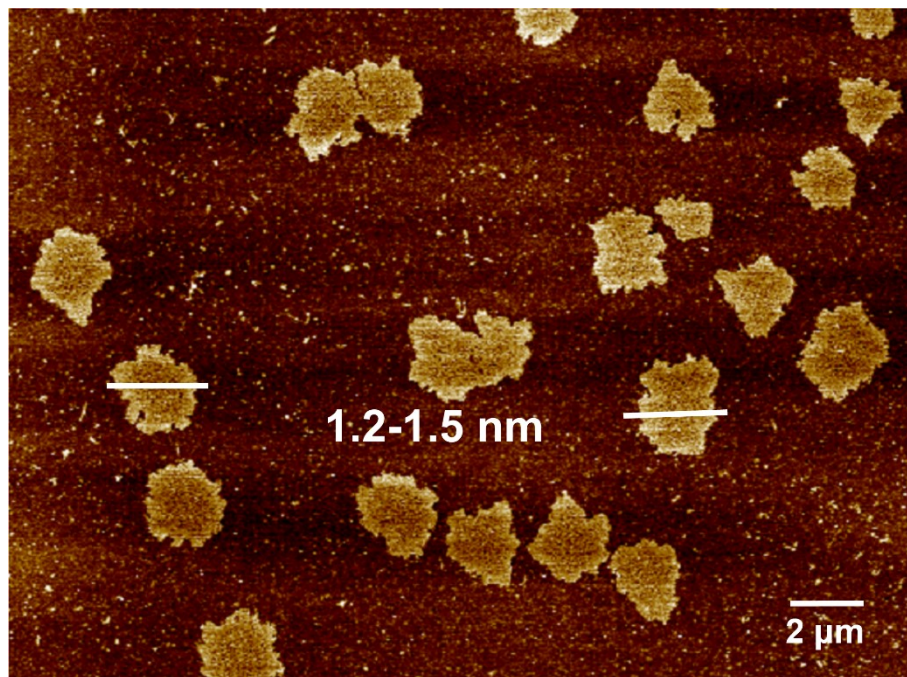


Figure S3. AFM image of XAIU-5-NS.

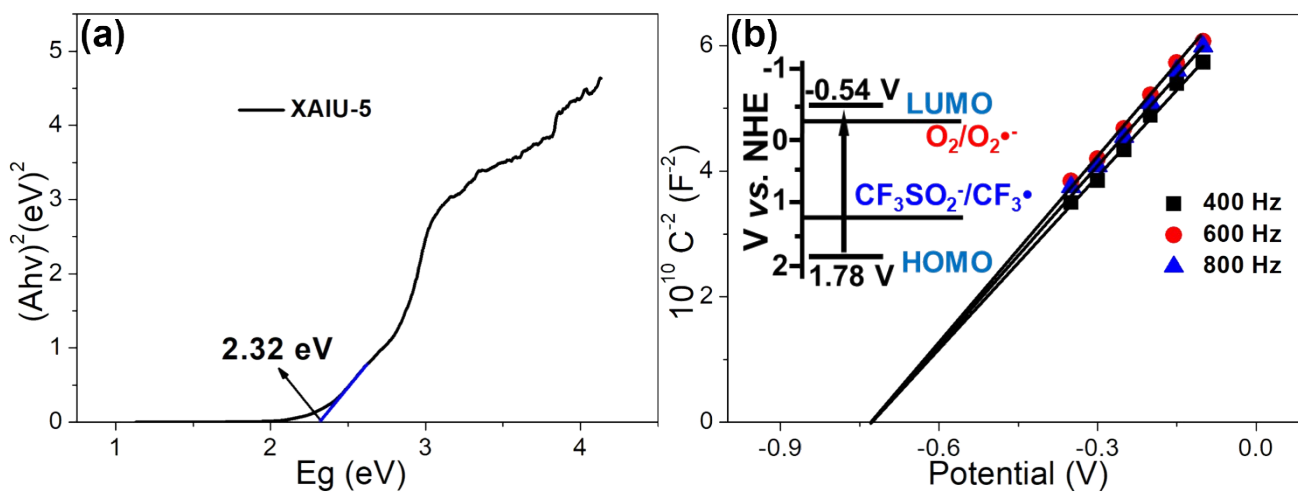


Figure S4. (a) The Tauc plot of XAIU-5; (b) the Mott-Schottky plots for XAIU-5 in 0.2 mol/L Na_2SO_4 aqueous solution.

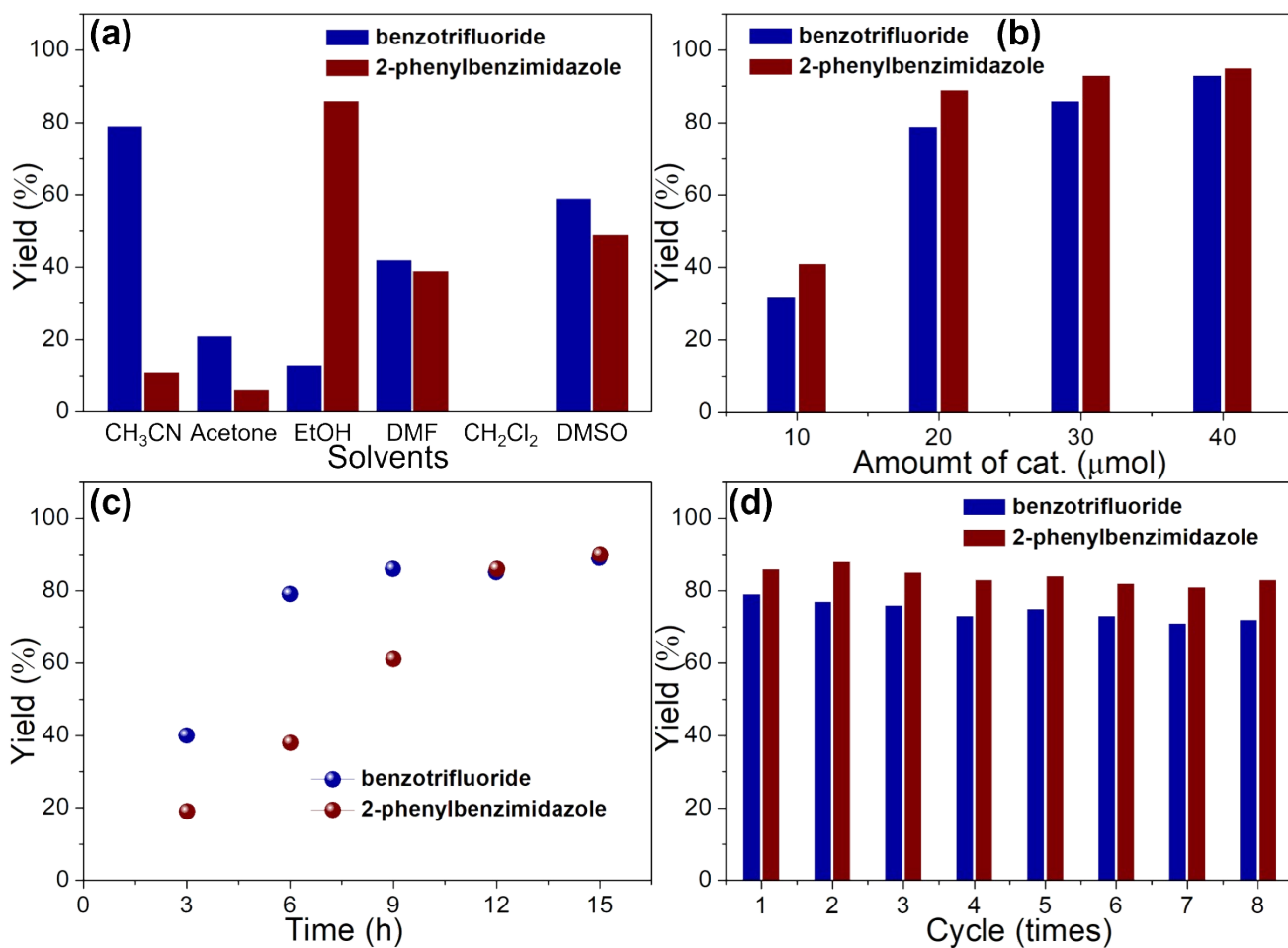


Figure S5. (a) Yields of benzotrifluoride and 2-phenylbenzimidazole in different solvents; (b) the influence of photocatalyst amounts in photocatalytic reactions; (c) the influence of irradiation time on the yield of benzotrifluoride and 2-phenylbenzimidazole of **XAIU-5-NS**; (d) cycling runs for the photocatalytic trifluoromethylation reaction and the sequential oxidation–cyclisation reaction in the presence of **XAIU-5-NS**.

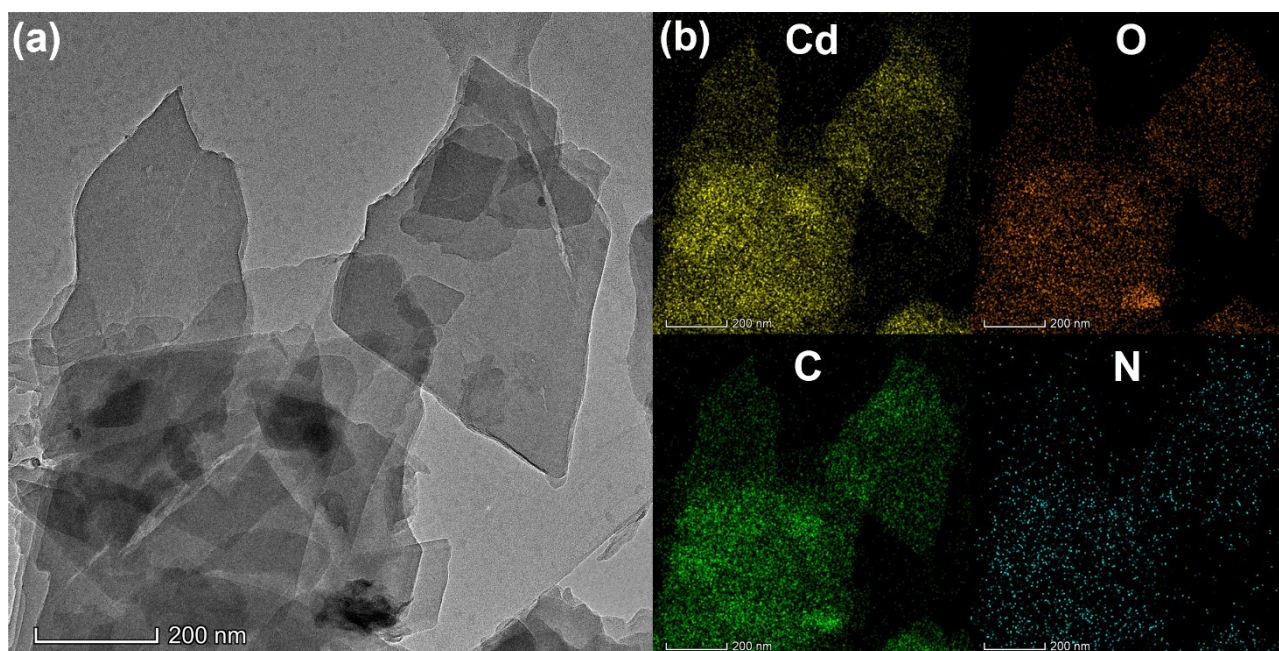


Figure S6. (a) The TEM image of **XAIU-5-NS** after eight cycles of reaction; (b) TEM mapping images of **XAIU-5-NS** after eight cycles of reaction.

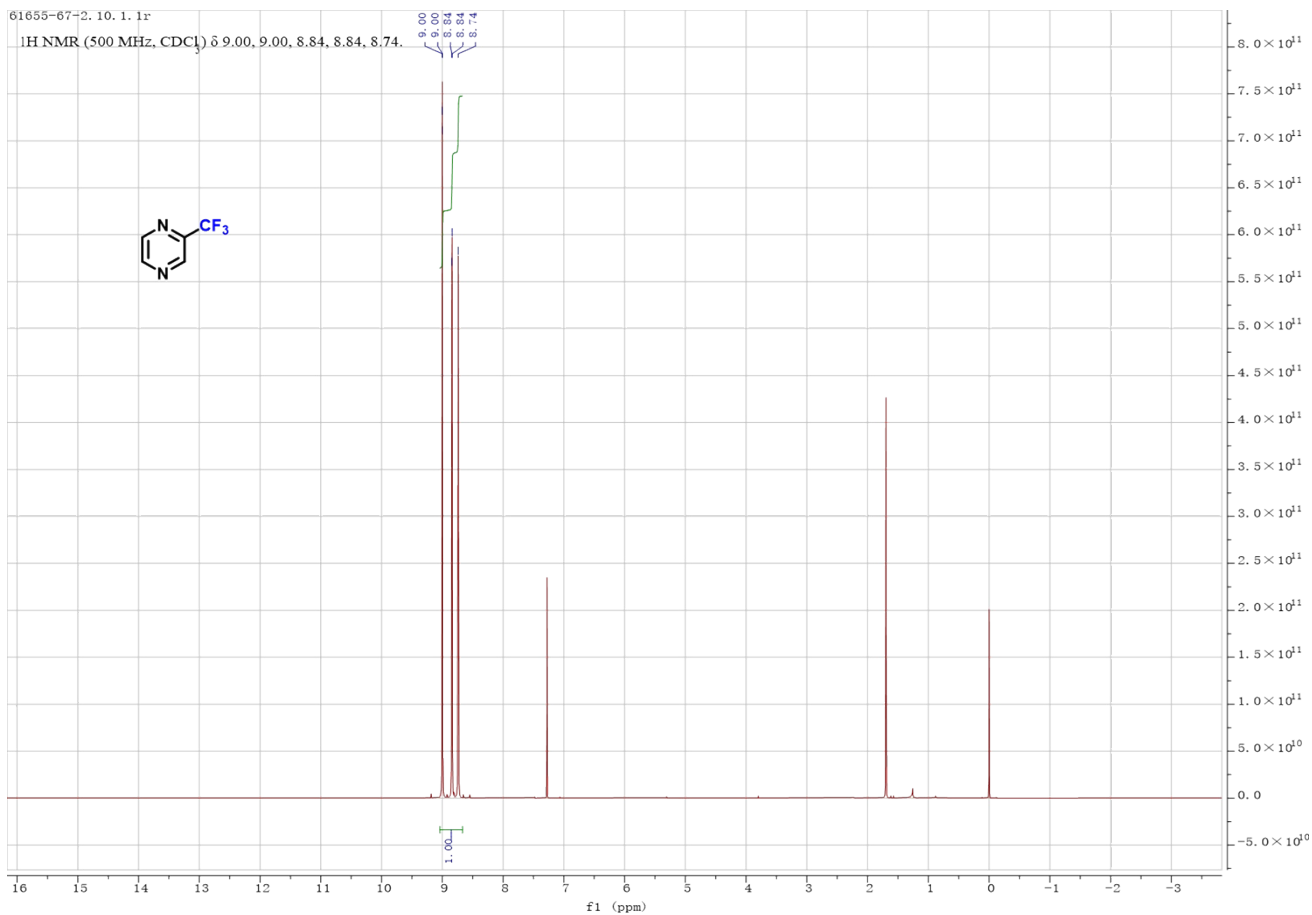
NMR Data of Products

Separation process for target products

After reaction, solvent not participating in the reaction was removed under reduced pressure. The crude products were purified by $\text{SiO}_2/\text{Al}_2\text{O}_3$ column chromatography using acetic ether and petroleum ether (V:V=1:1) as an eluent so that the white solids acylamide derivatives can be obtained. 0.25 mm silica gelcoated glass plates were used in the thin layer chromatography (TLC).

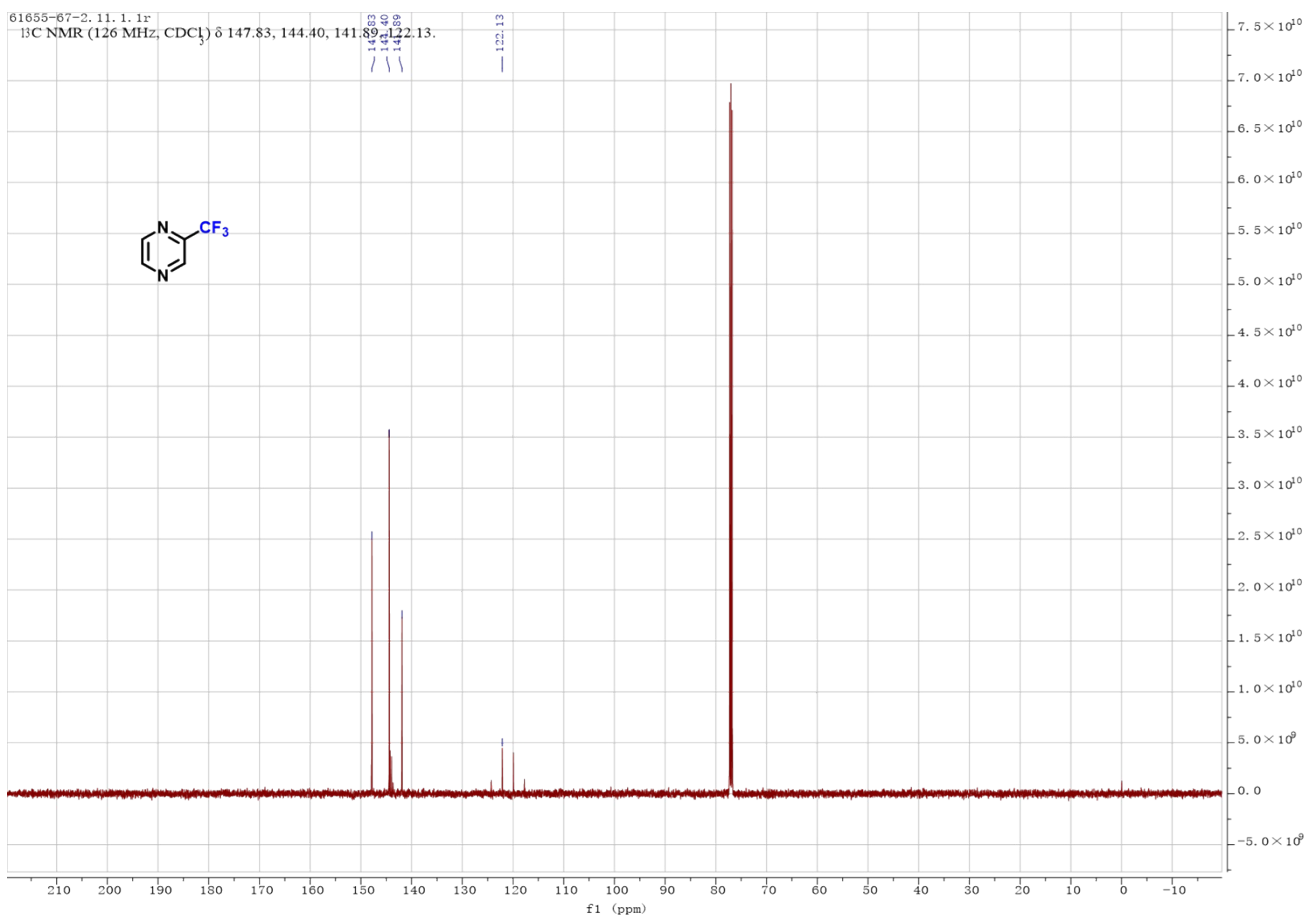
61655-67-2. 10. 1. 1r

¹H NMR (500 MHz, CDCl₃) δ 9.00, 9.00, 8.84, 8.84, 8.74.



61655-67-2. 11. 1. 1r

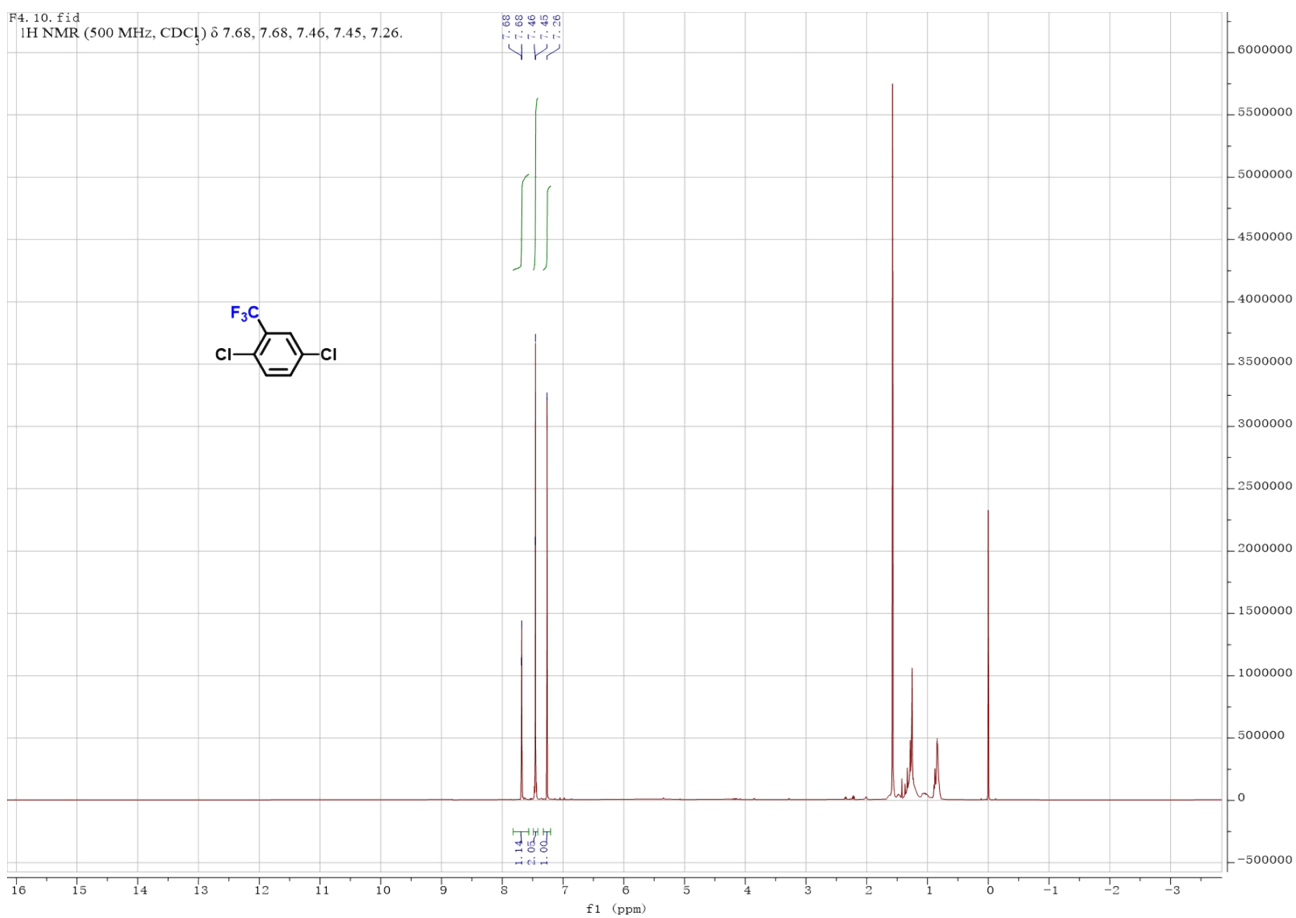
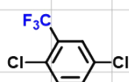
¹³C NMR (126 MHz, CDCl₃) δ 147.83, 144.40, 141.89, 141.89, 122.13.



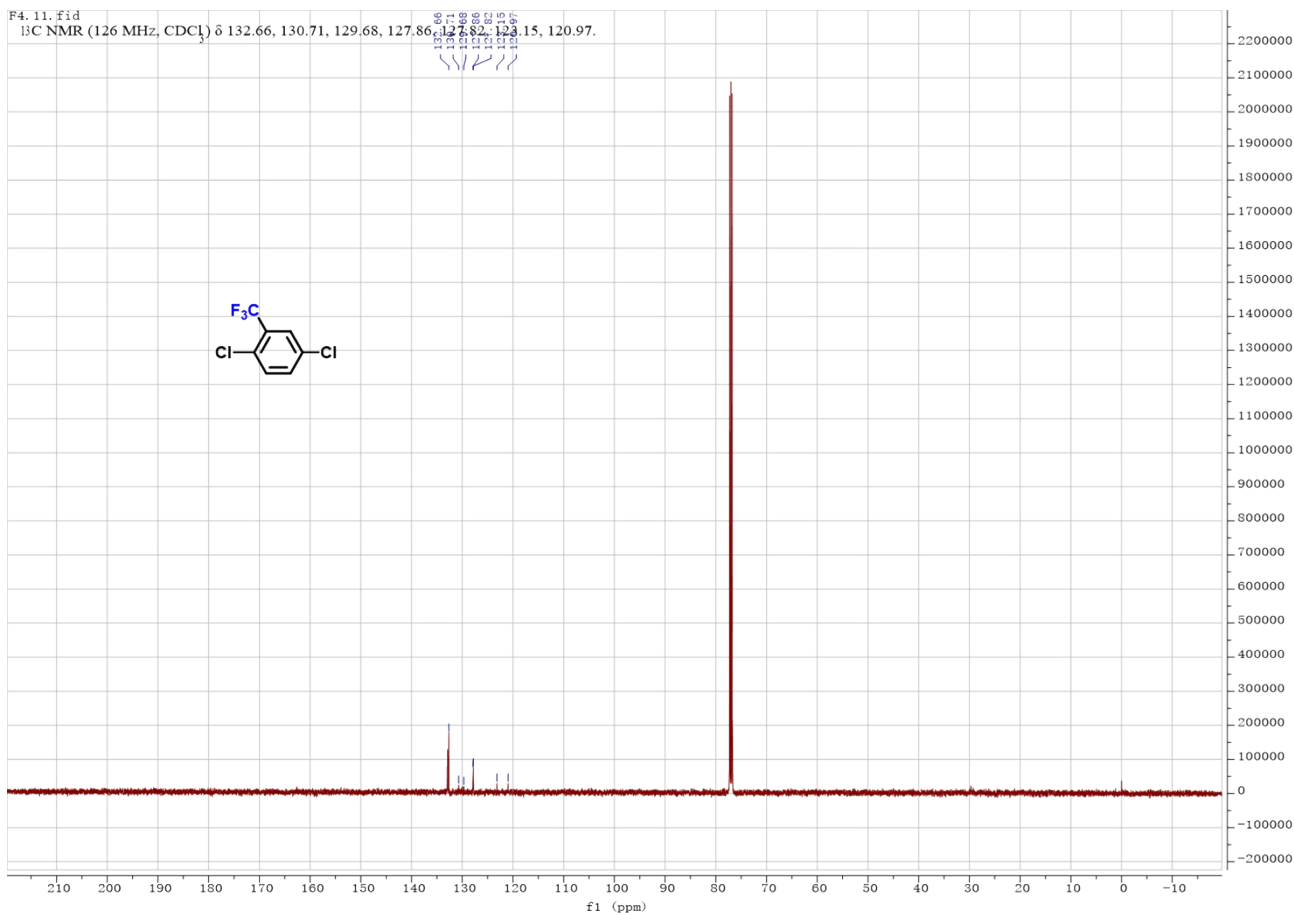
61655-67-2. 12. 1. 1r
19F NMR (471 MHz, CDCl₃) δ -67.86.



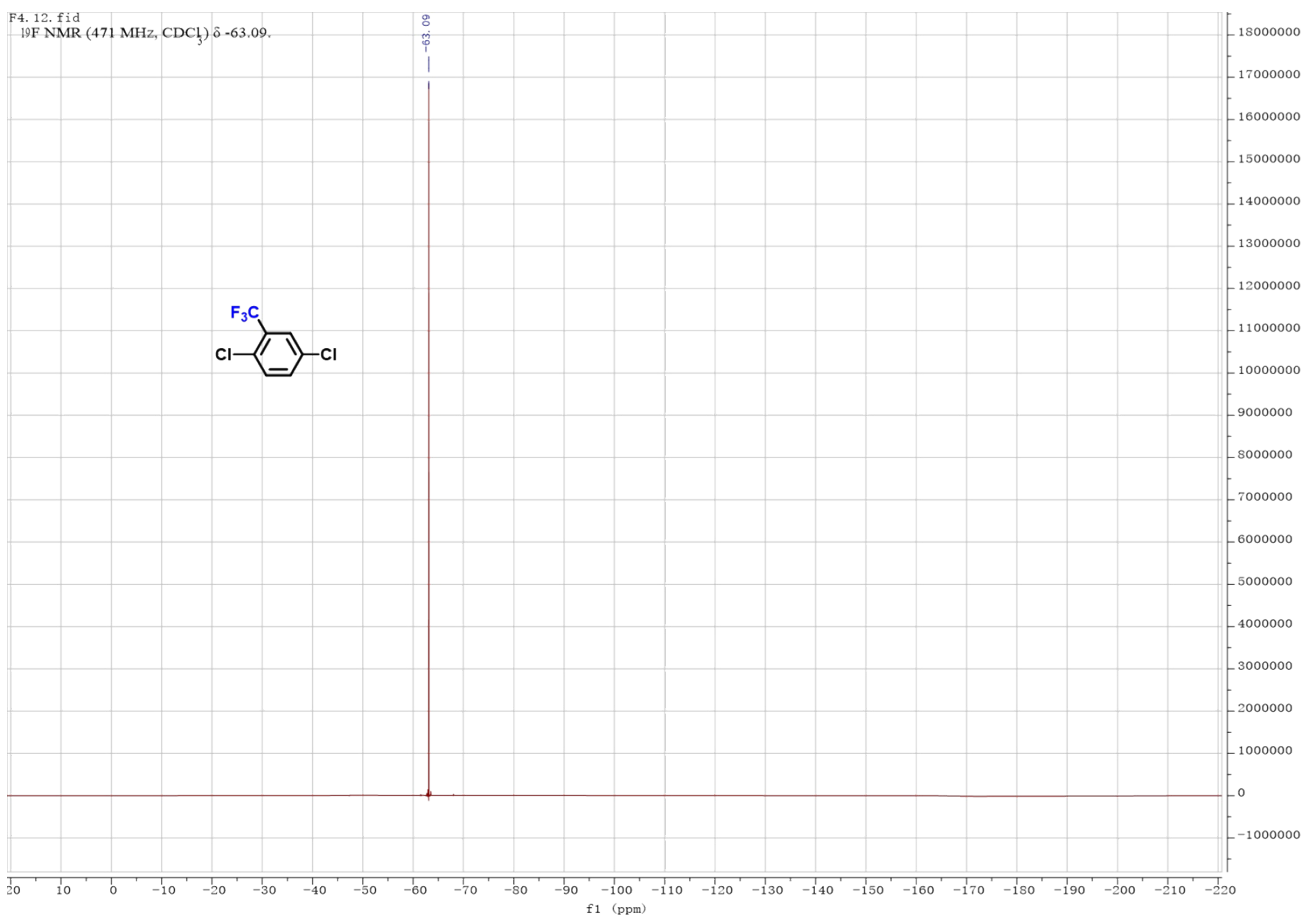
F4. 10. fid
1H NMR (500 MHz, CDCl₃) δ 7.68, 7.68, 7.46, 7.45, 7.26.

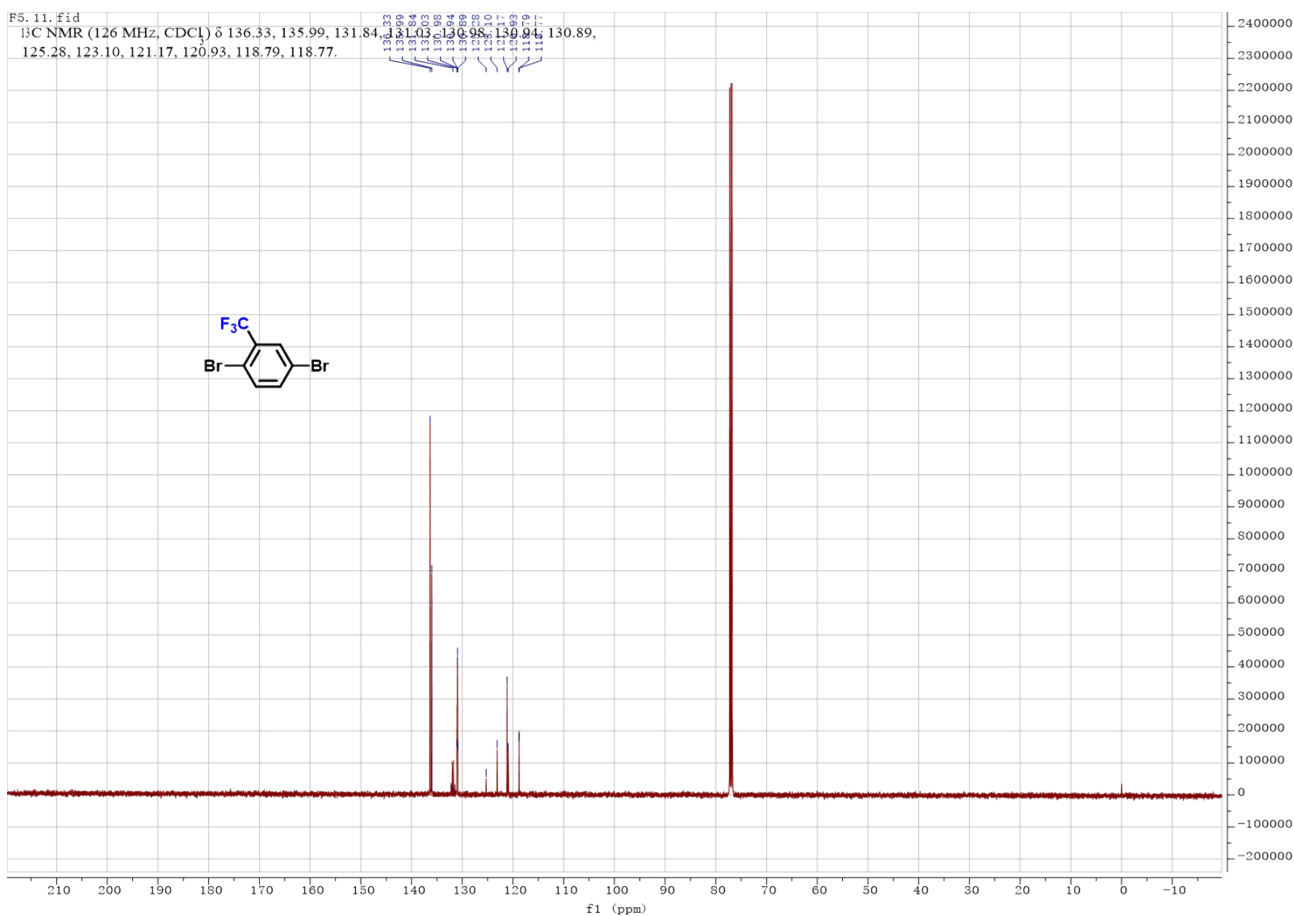
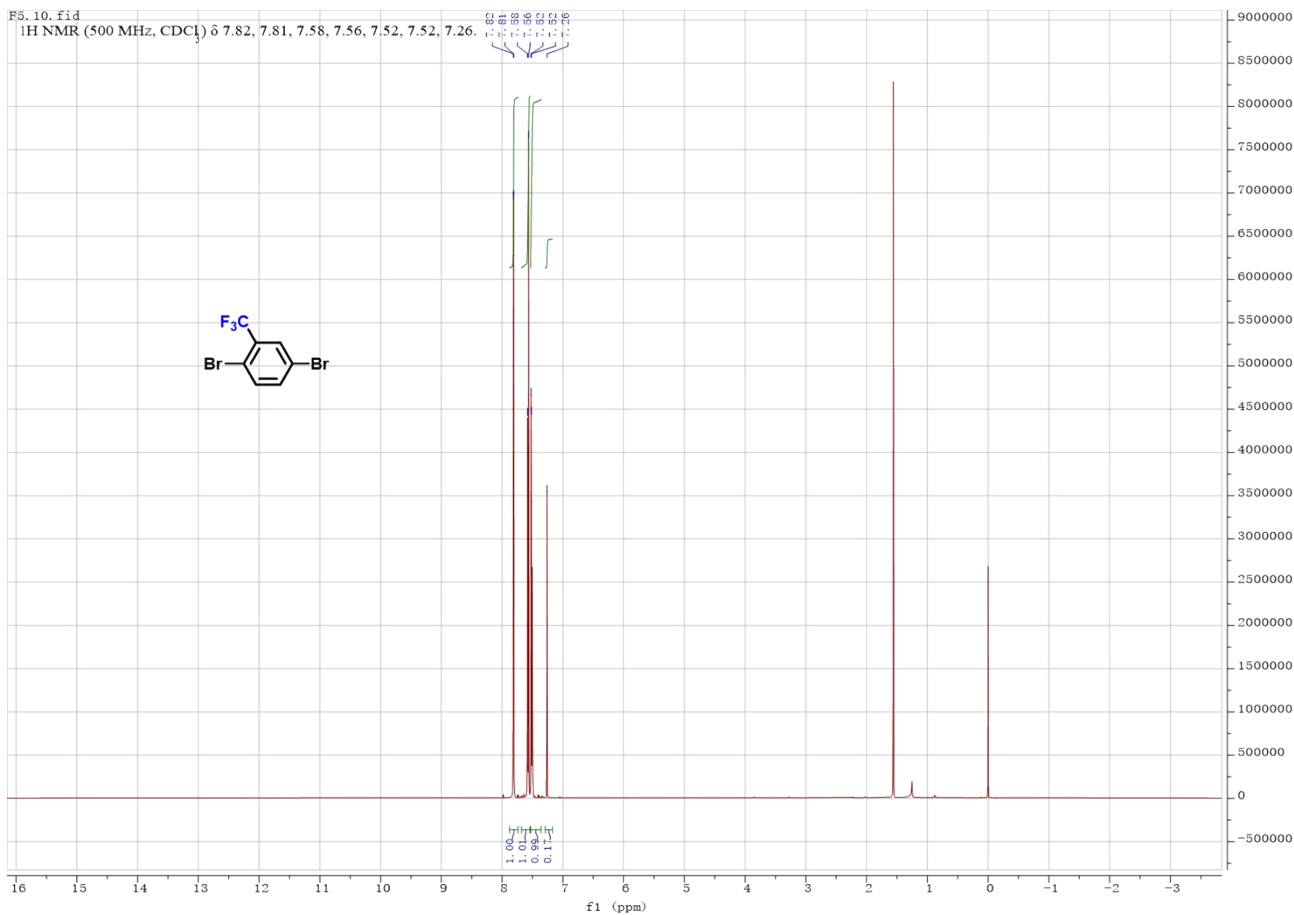


F4.11.fid
¹³C NMR (126 MHz, CDCl₃) δ 132.66, 130.71, 129.68, 127.86, 127.82, 123.15, 120.97.

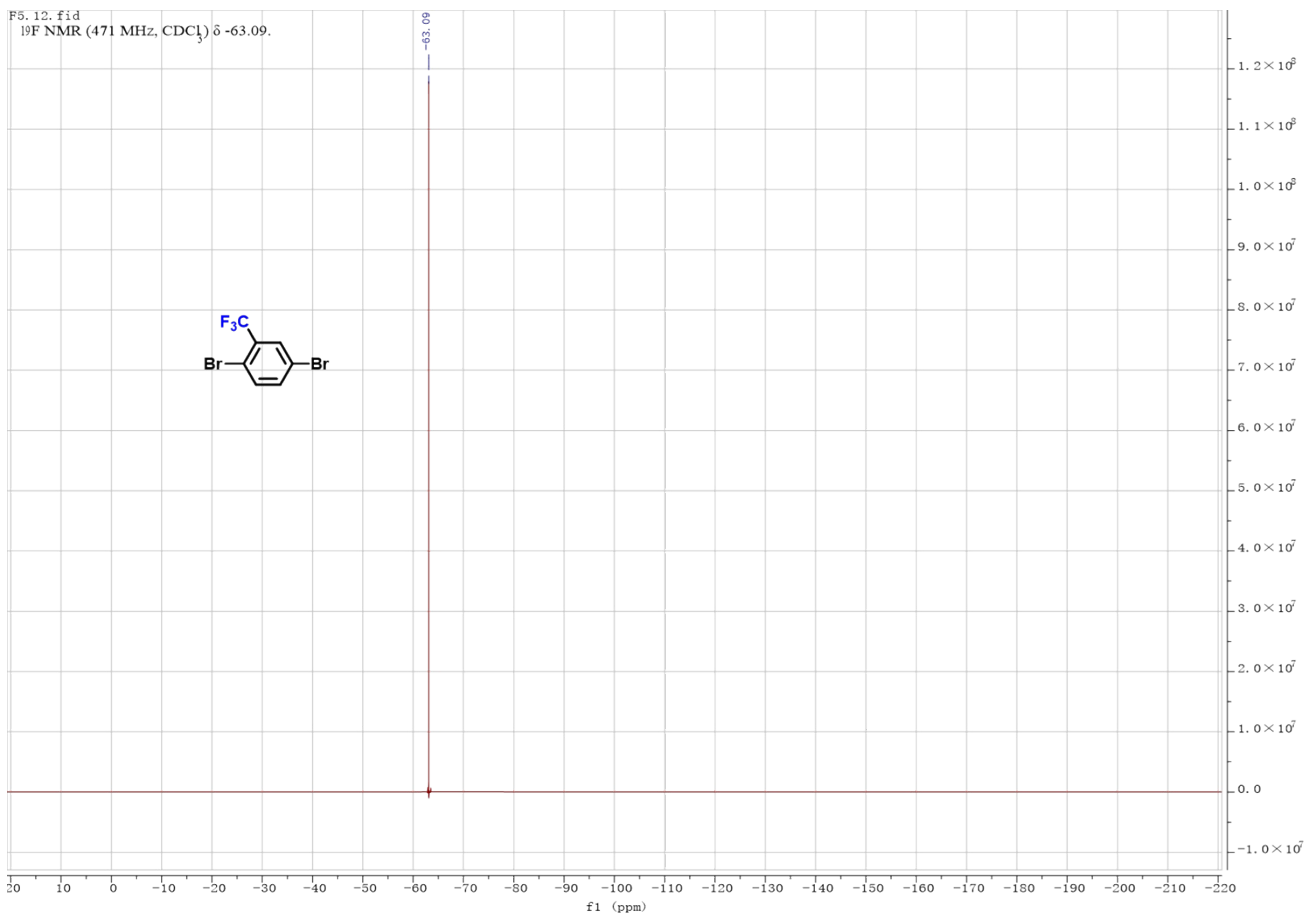


F4.12.fid
¹⁹F NMR (471 MHz, CDCl₃) δ -63.09.

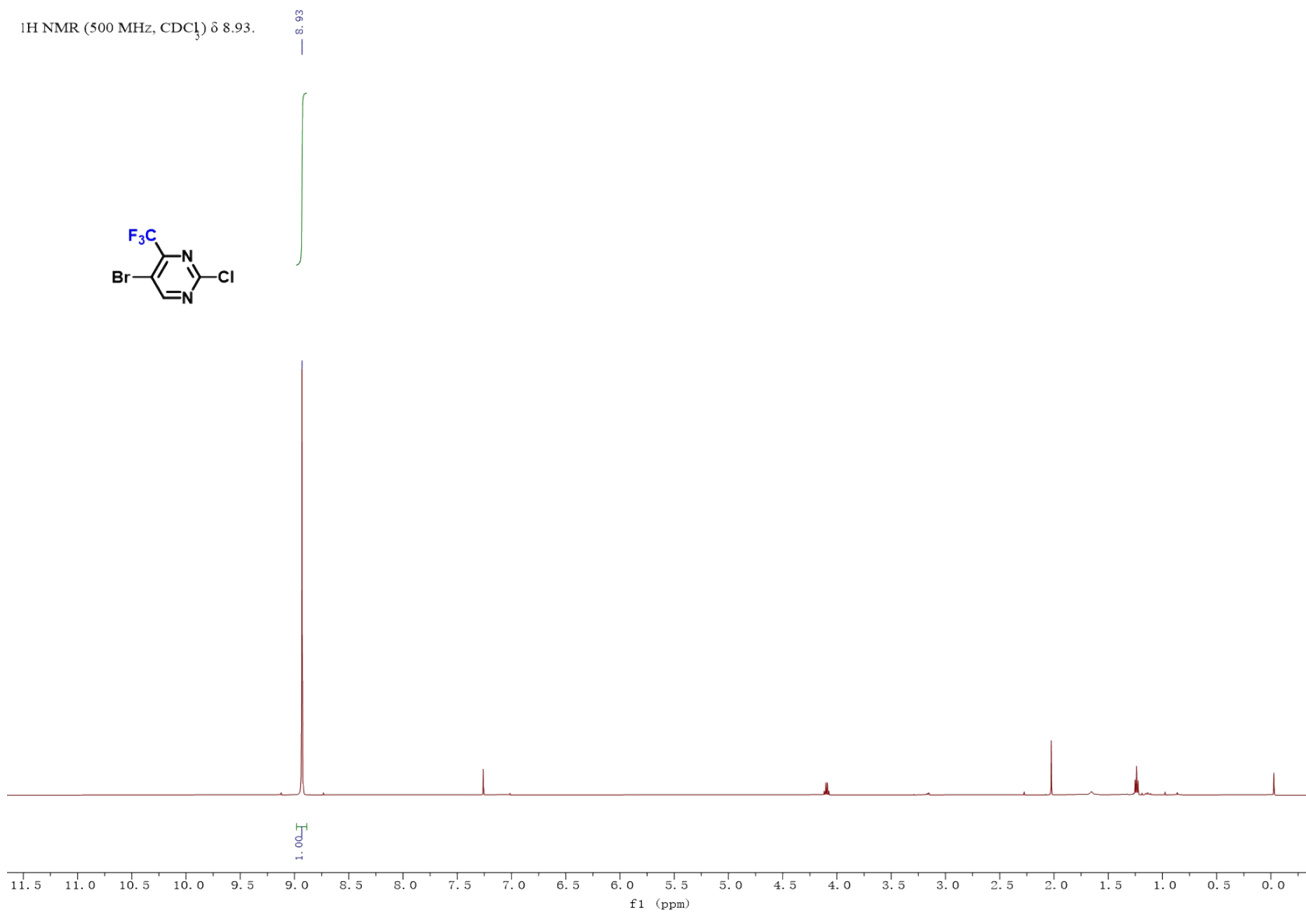




F5_12.fid
¹⁹F NMR (471 MHz, CDCl₃) δ -63.09.



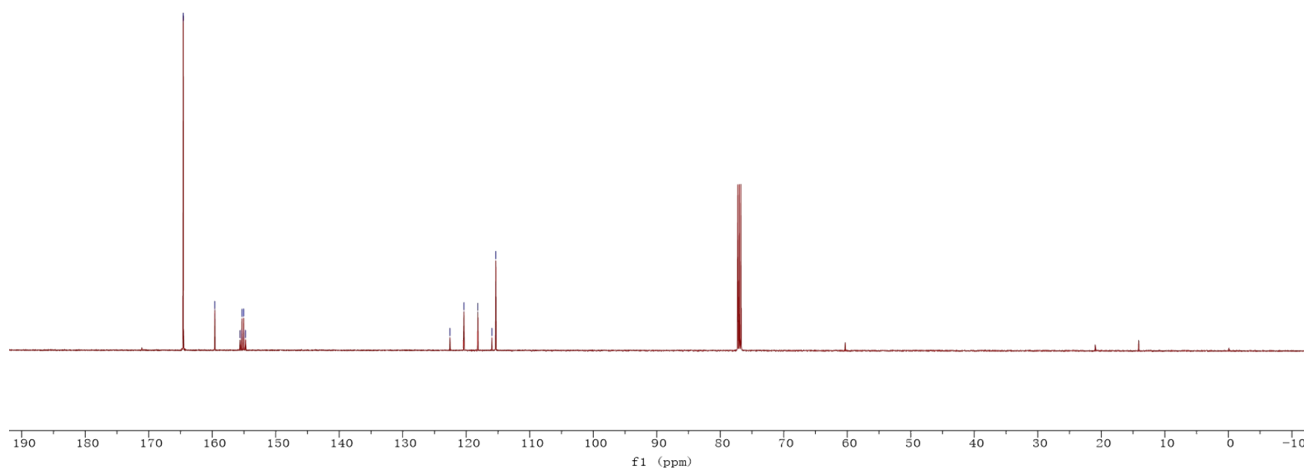
¹H NMR (500 MHz, CDCl₃) δ 8.93.



164.56
159.60
155.63
155.33
155.04
154.75

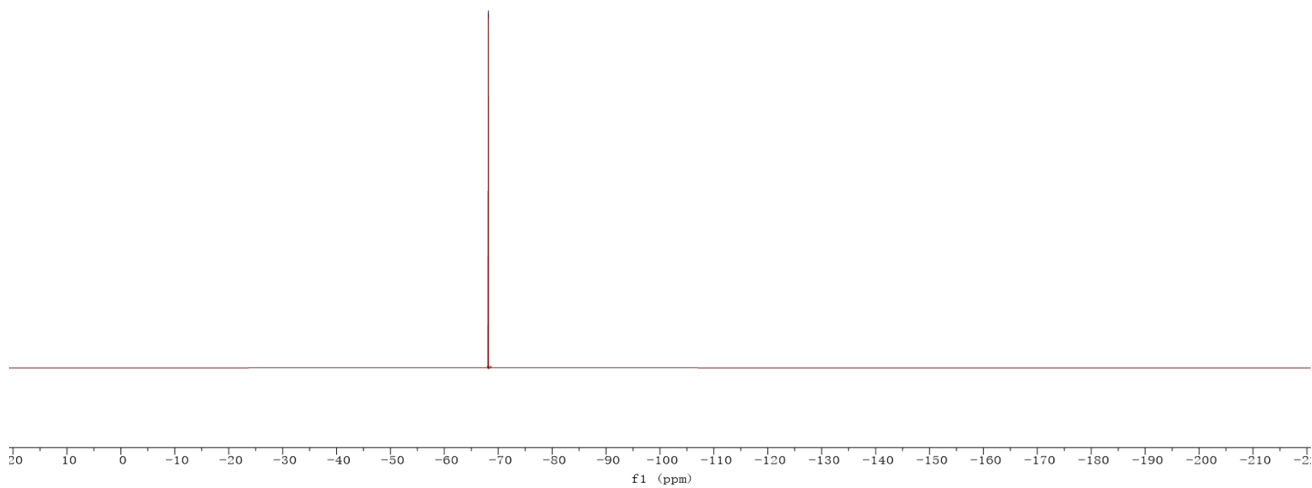
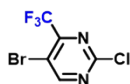
122.88
120.89
118.97
118.34

^{13}C NMR (126 MHz, CDCl_3) δ 164.56, 159.60, 155.63, 155.33, 155.04, 154.75, 122.58, 120.38, 118.17, 115.97, 115.34.



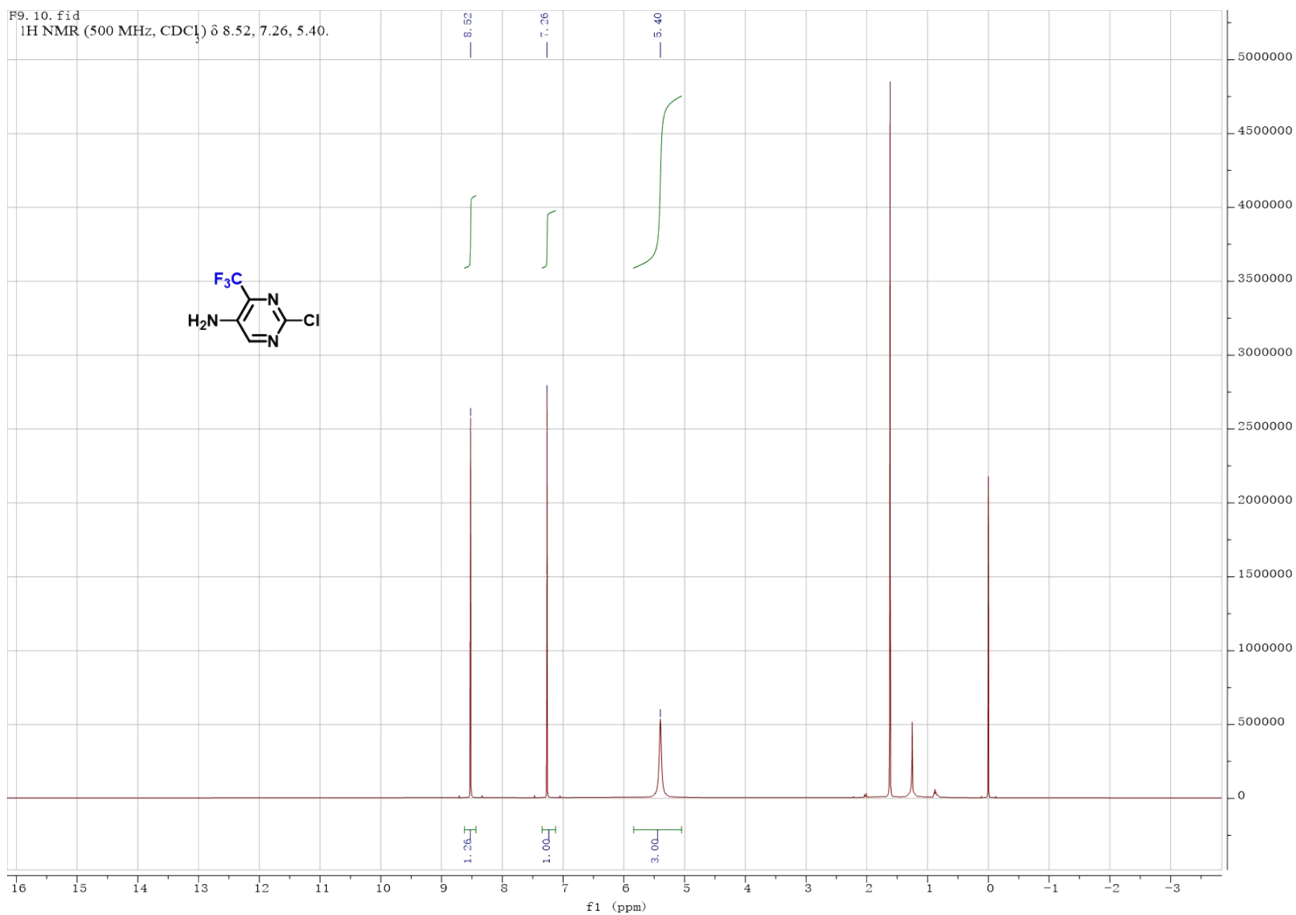
^{19}F NMR (471 MHz, CDCl_3) δ -68.20.

-68.20



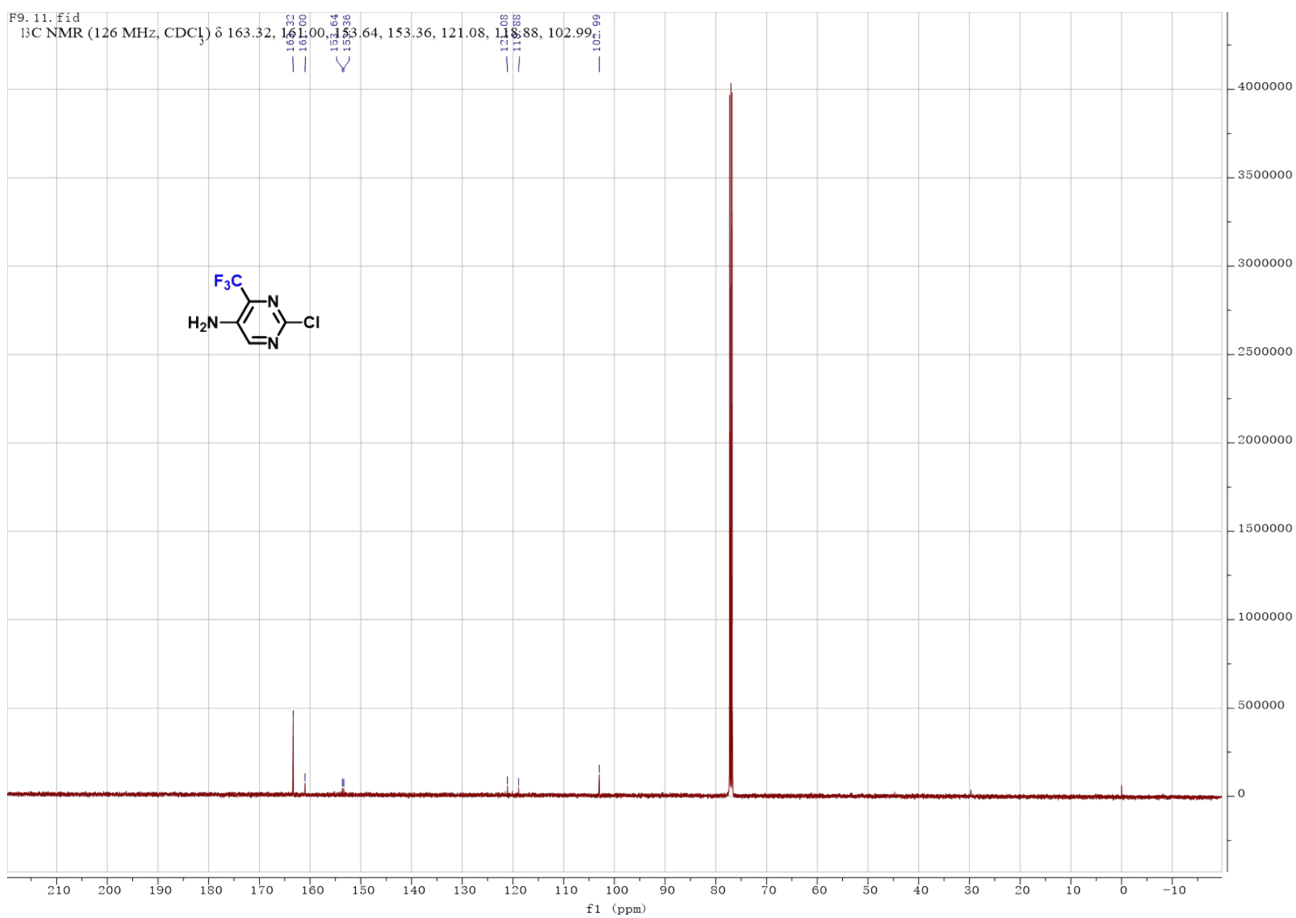
F9_10.fid

¹H NMR (500 MHz, CDCl₃) δ 8.52, 7.26, 5.40.

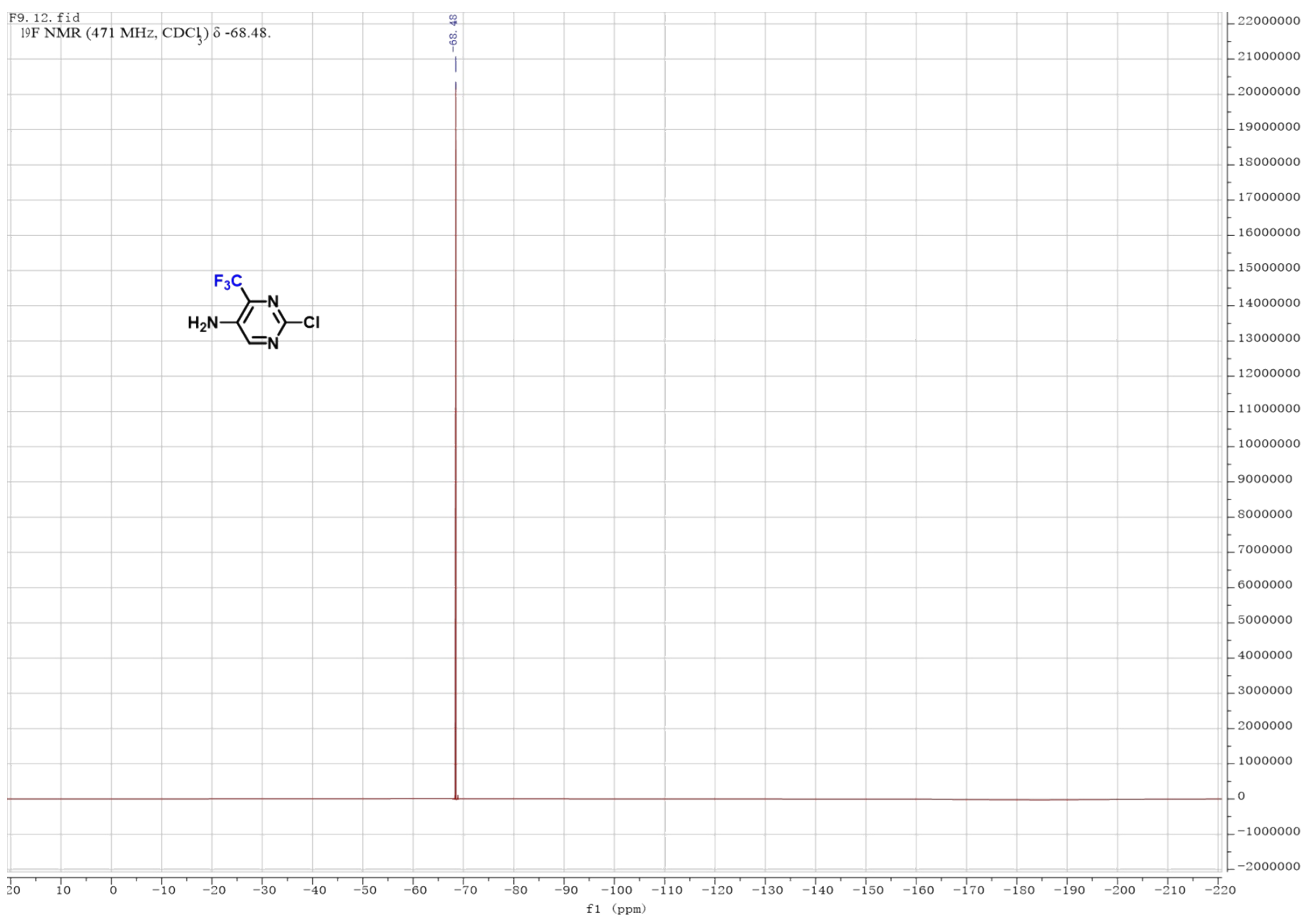


F9_11.fid

¹³C NMR (126 MHz, CDCl₃) δ 163.32, 161.00, 153.64, 153.36, 153.36, 121.08, 118.88, 102.99.



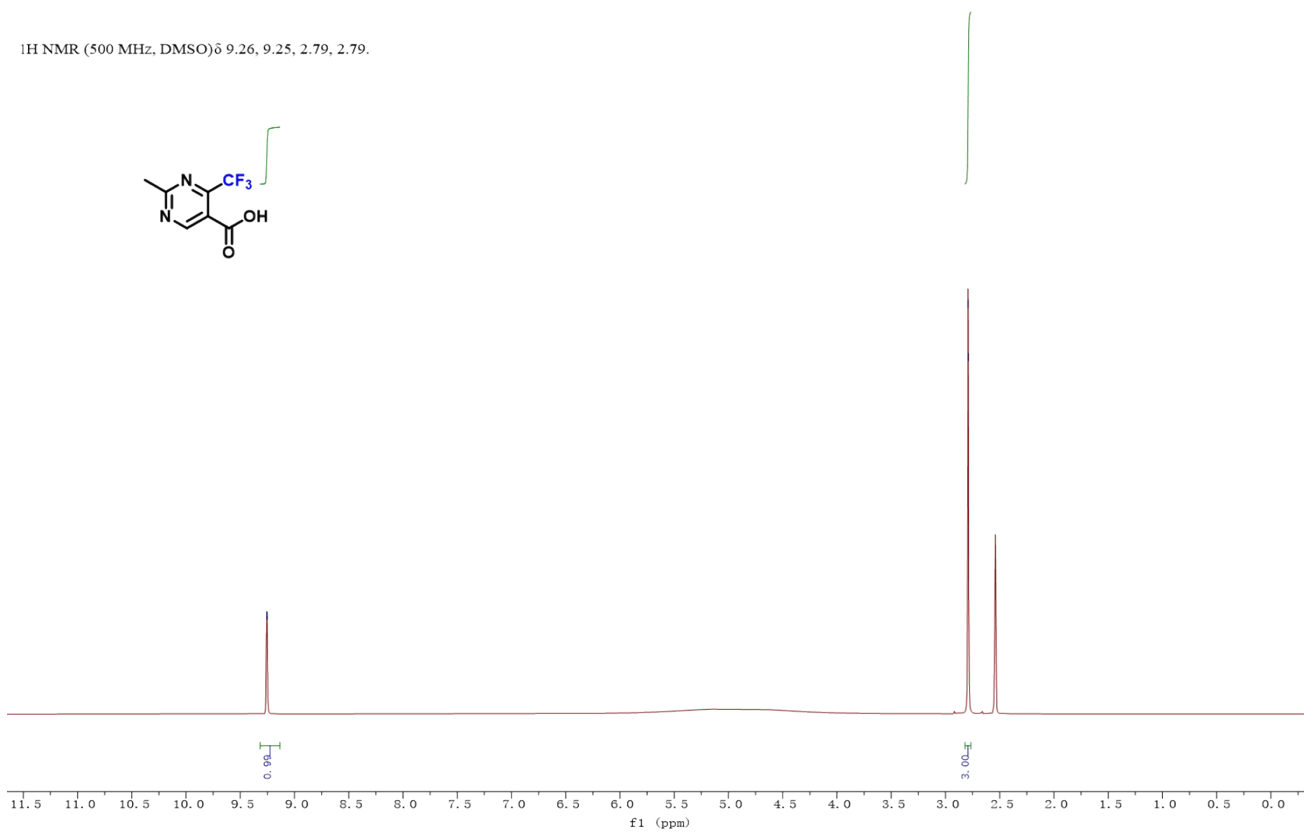
F9_12.fid
¹⁹F NMR (471 MHz, CDCl₃) δ -68.48.



9.26
9.25

2.79
2.79

¹H NMR (500 MHz, DMSO) δ 9.26, 9.25, 2.79, 2.79.

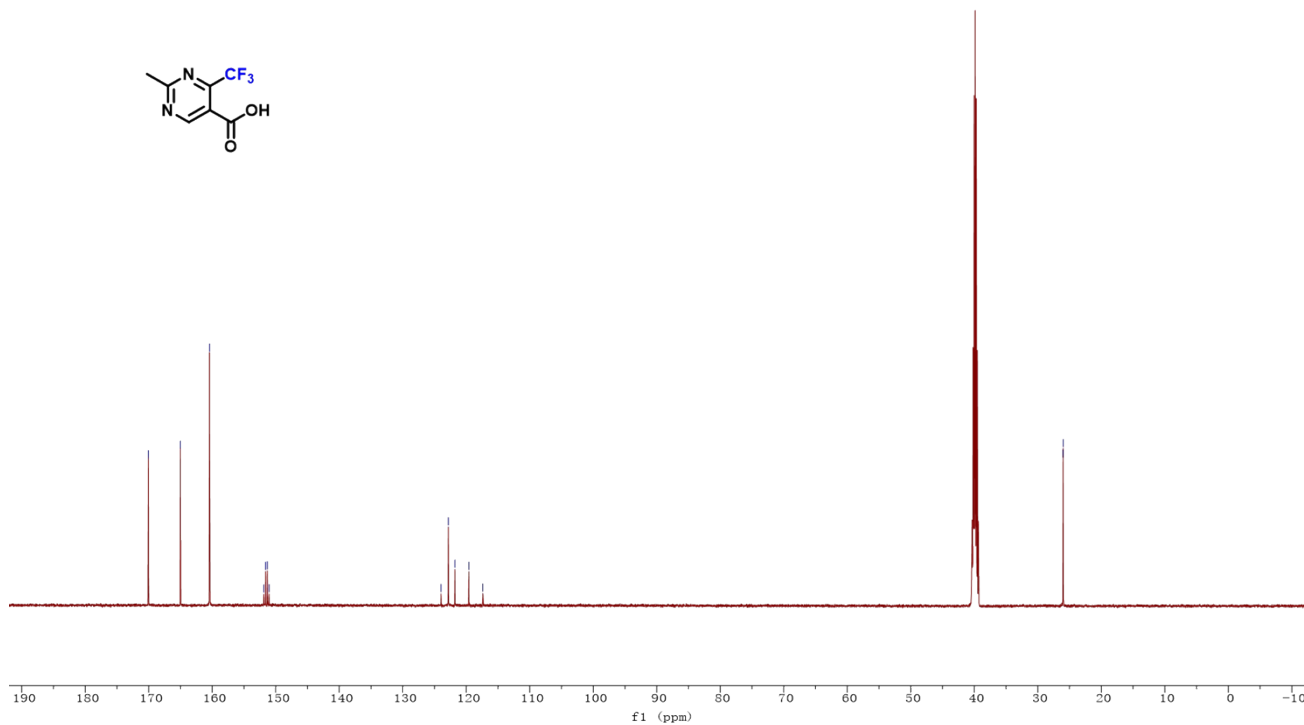
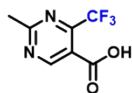


170.05
165.01
160.44
151.89
151.61
151.32
151.04

123.98
122.82
121.78
119.59
117.39

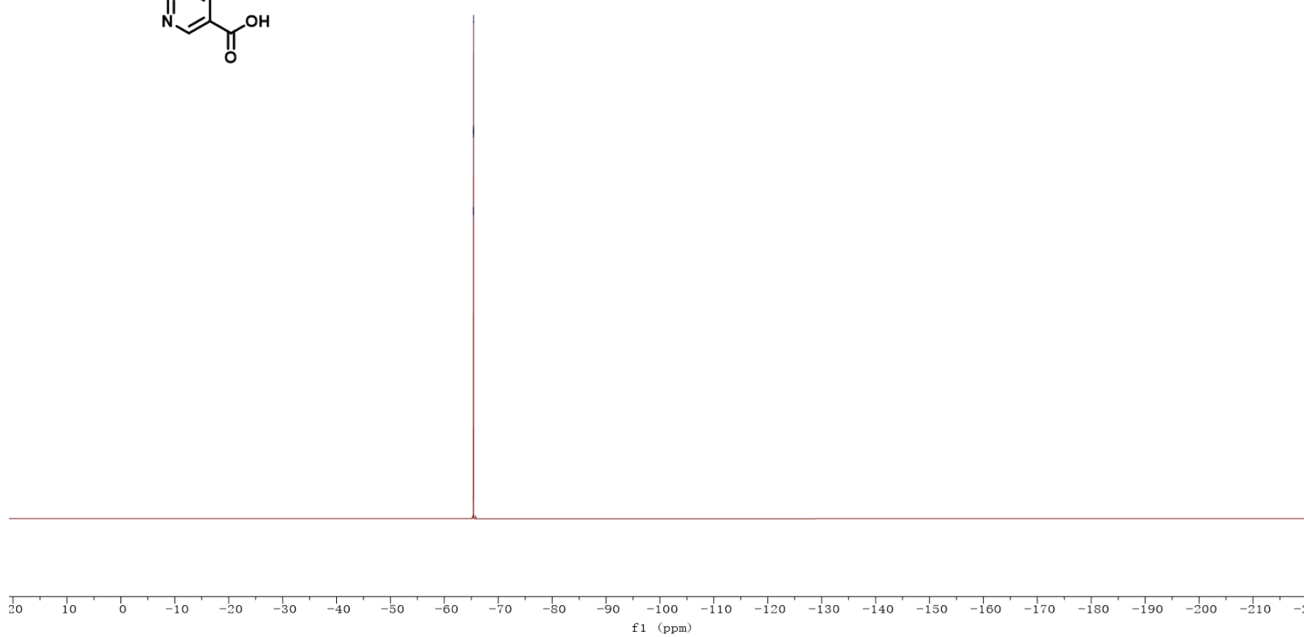
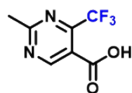
26.02
26.00

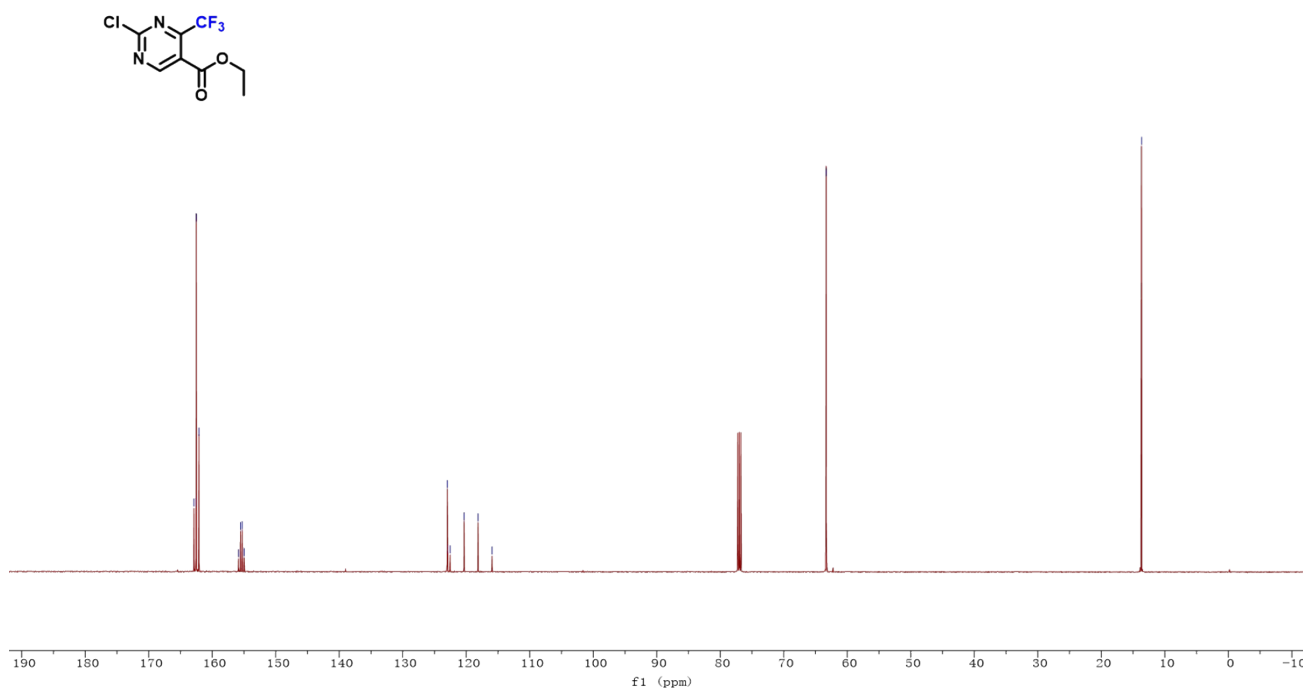
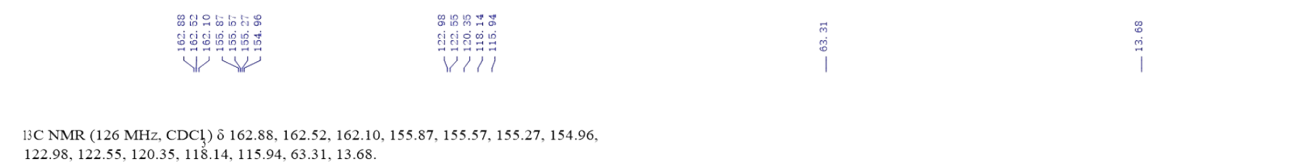
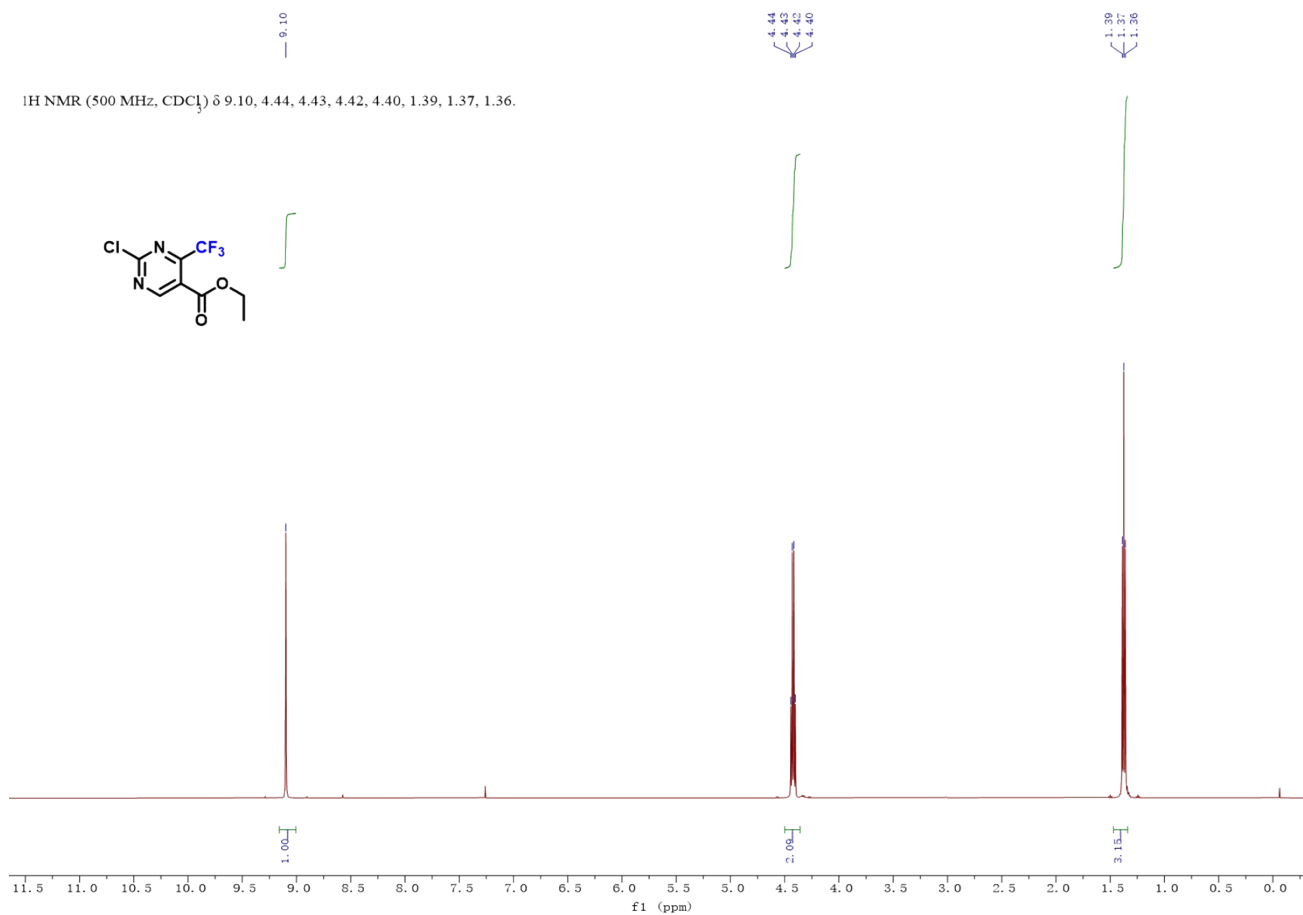
¹³C NMR (126 MHz, DMSO) δ 170.05, 165.01, 160.44, 151.89, 151.61, 151.32, 151.04, 123.98, 122.82, 121.78, 119.59, 117.39, 26.02, 26.00.



¹⁹F NMR (471 MHz, DMSO) δ -65.37, -65.38, -65.39, -65.41.

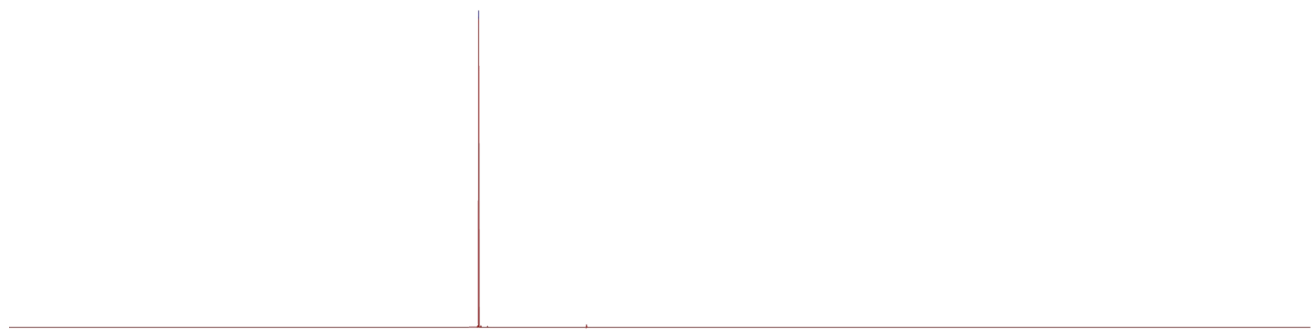
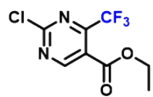
-65.37
-65.38
-65.39
-65.41





^{19}F NMR (471 MHz, CDCl_3) δ -66.37.

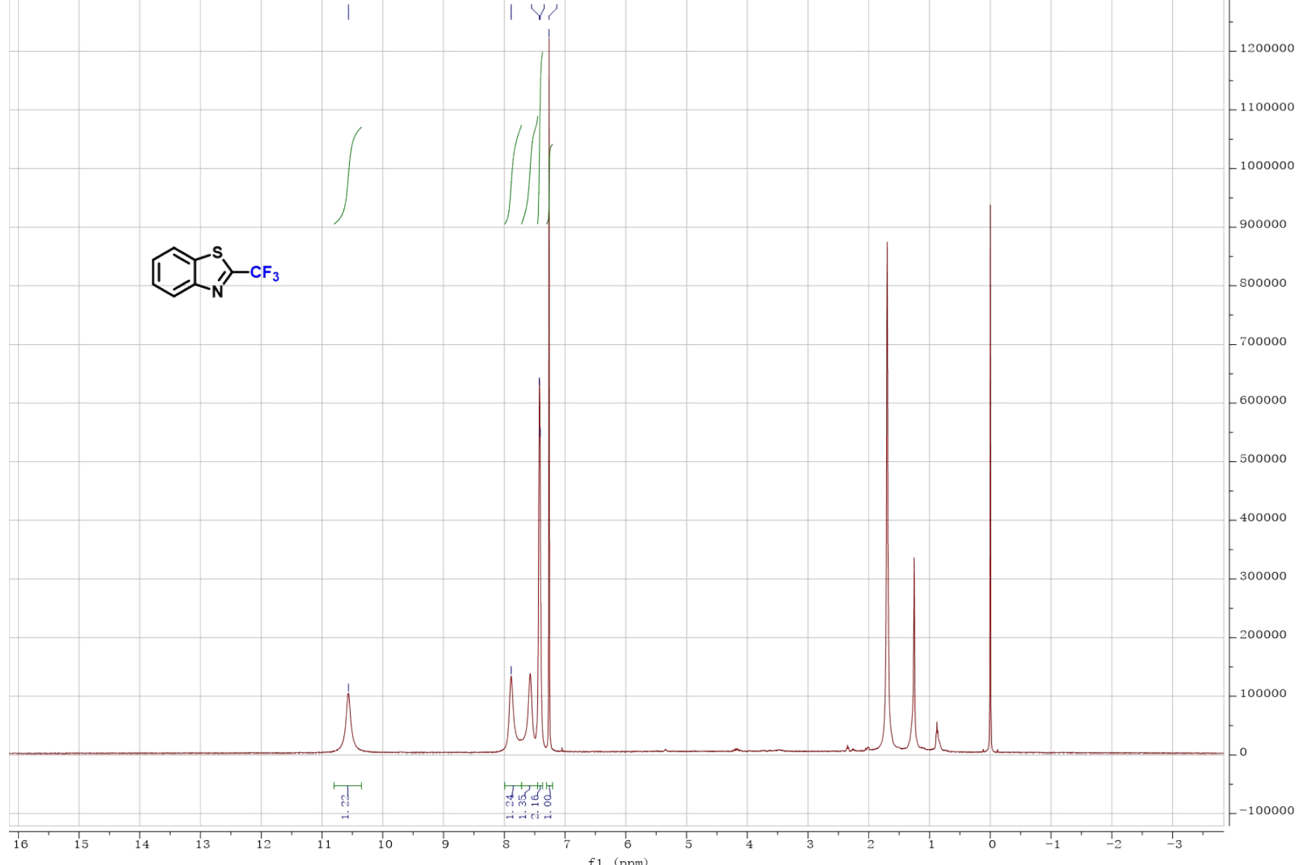
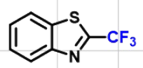
-66.37



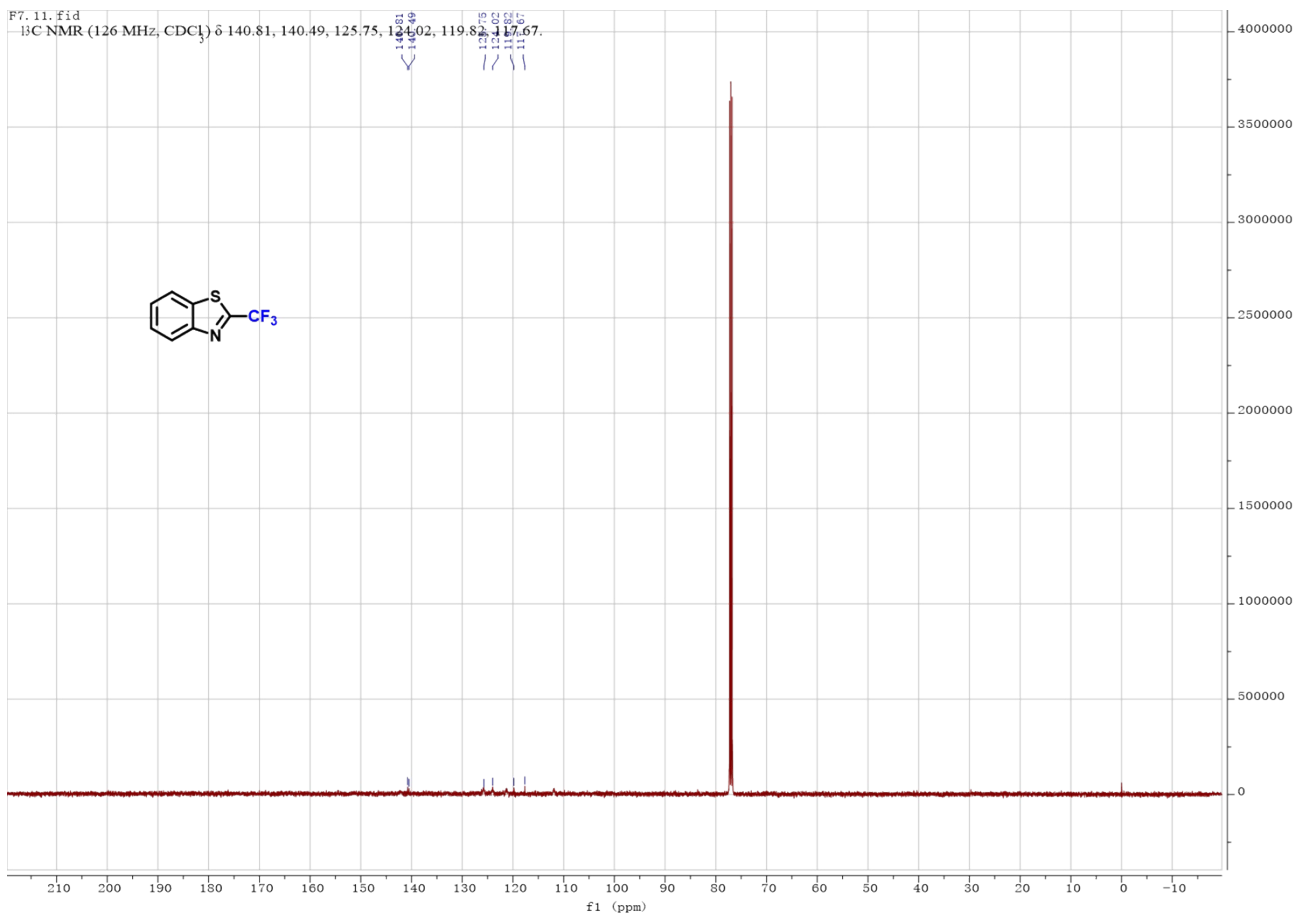
20 10 0 -10 -20 -30 -40 -50 -60 -70 -80 -90 -100 -110 -120 -130 -140 -150 -160 -170 -180 -190 -200 -210 -2

f1 (ppm)

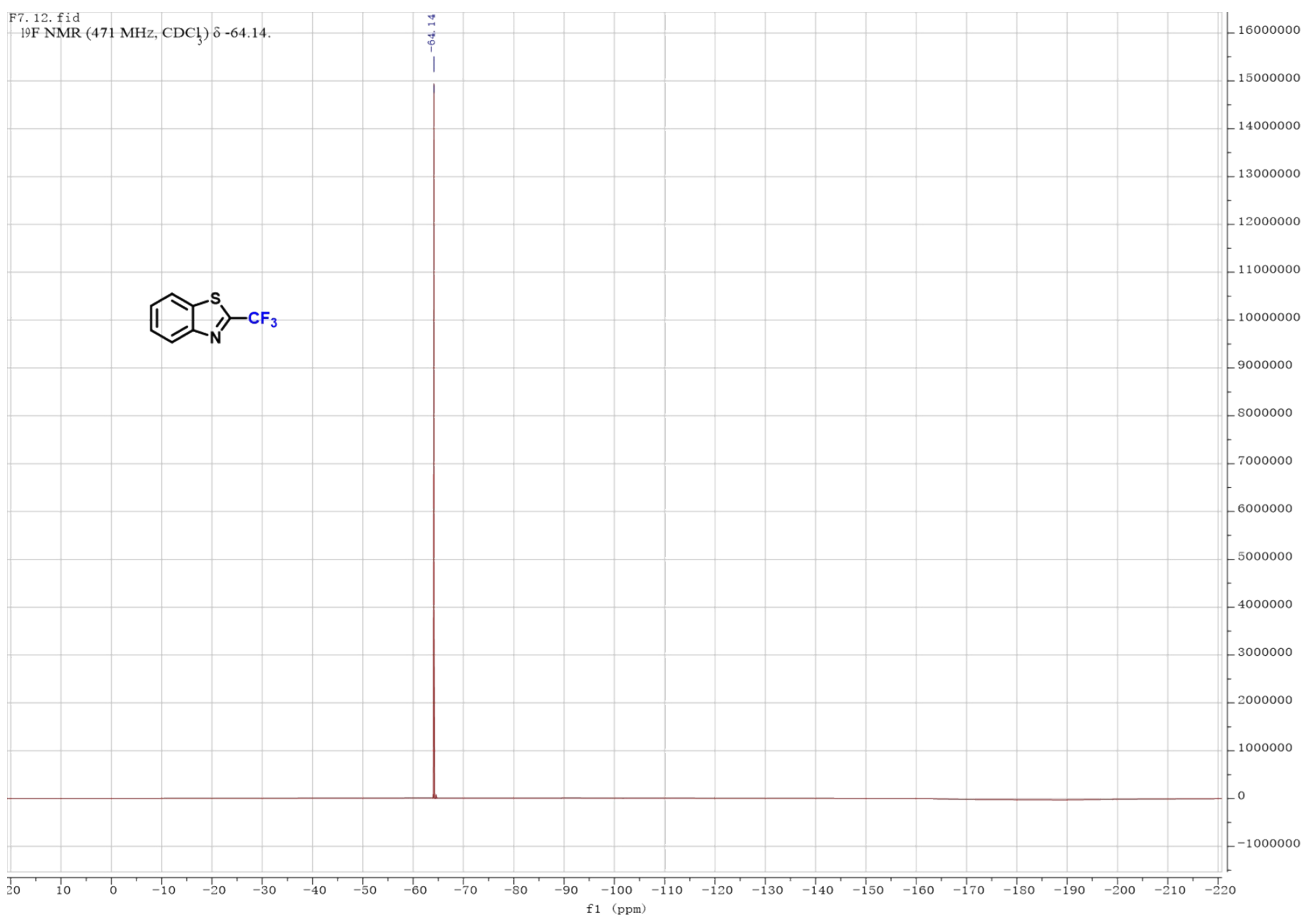
F7_10.fid
 ^1H NMR (500 MHz, CDCl_3) δ 10.57, 7.89, 7.42, 7.41, 7.26.

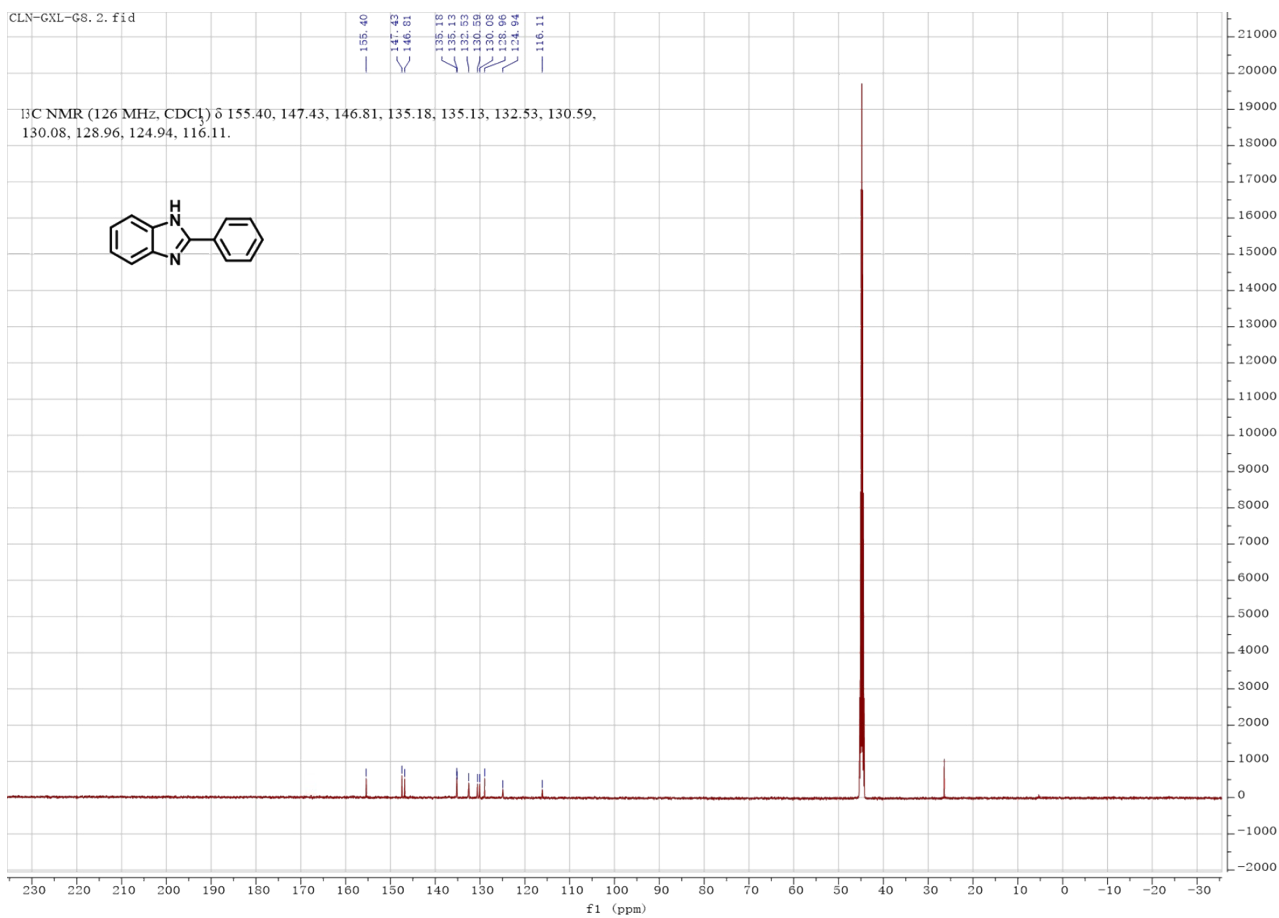
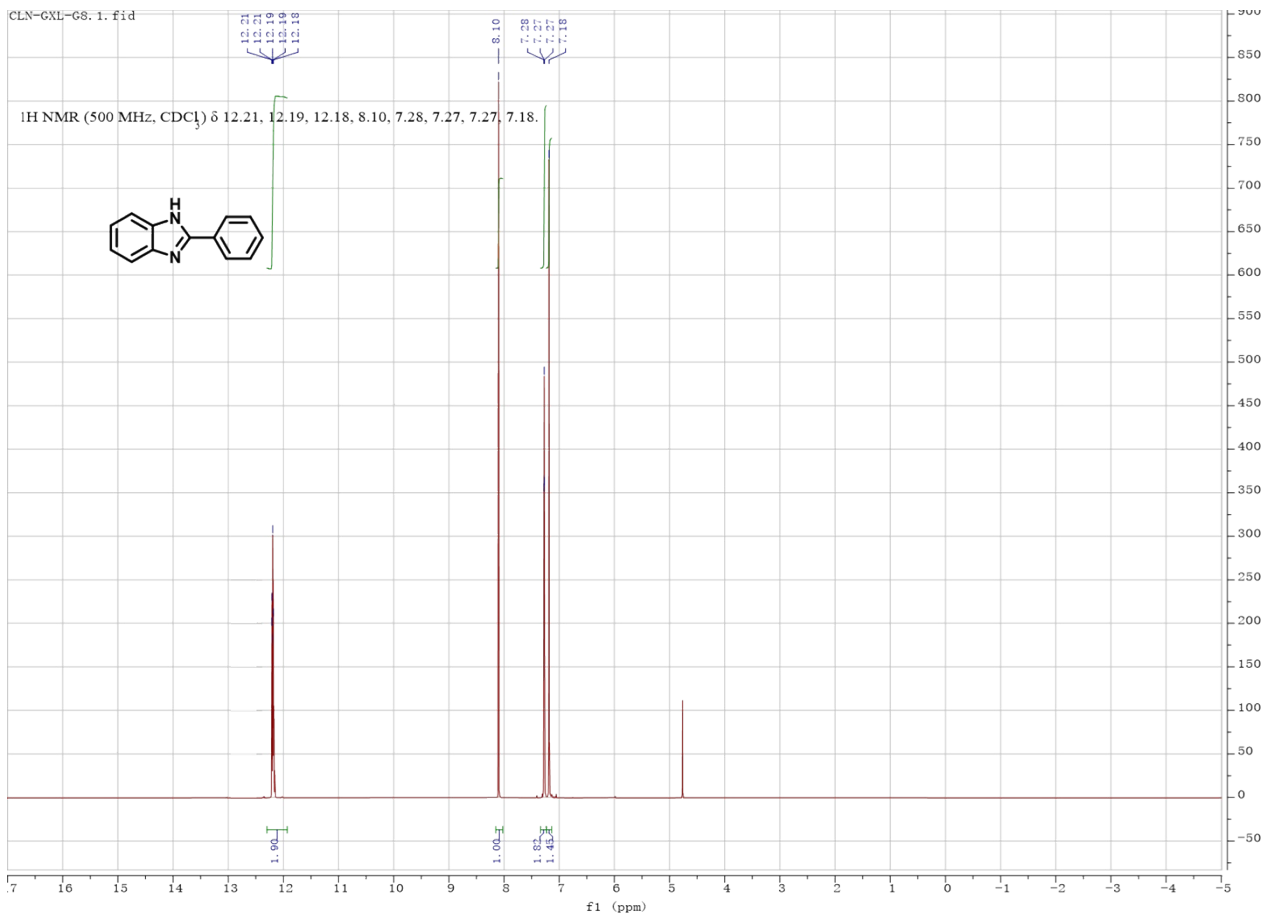


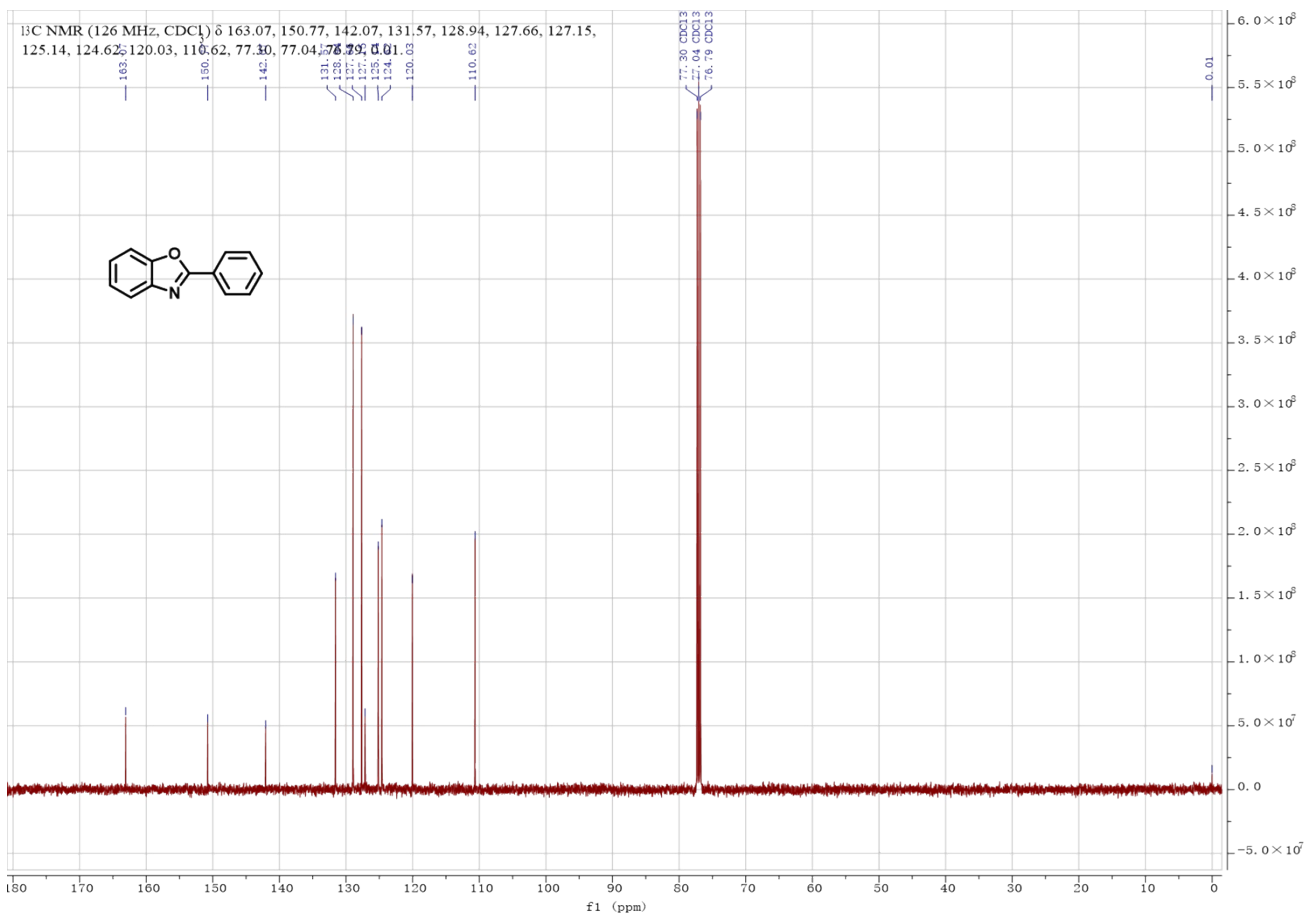
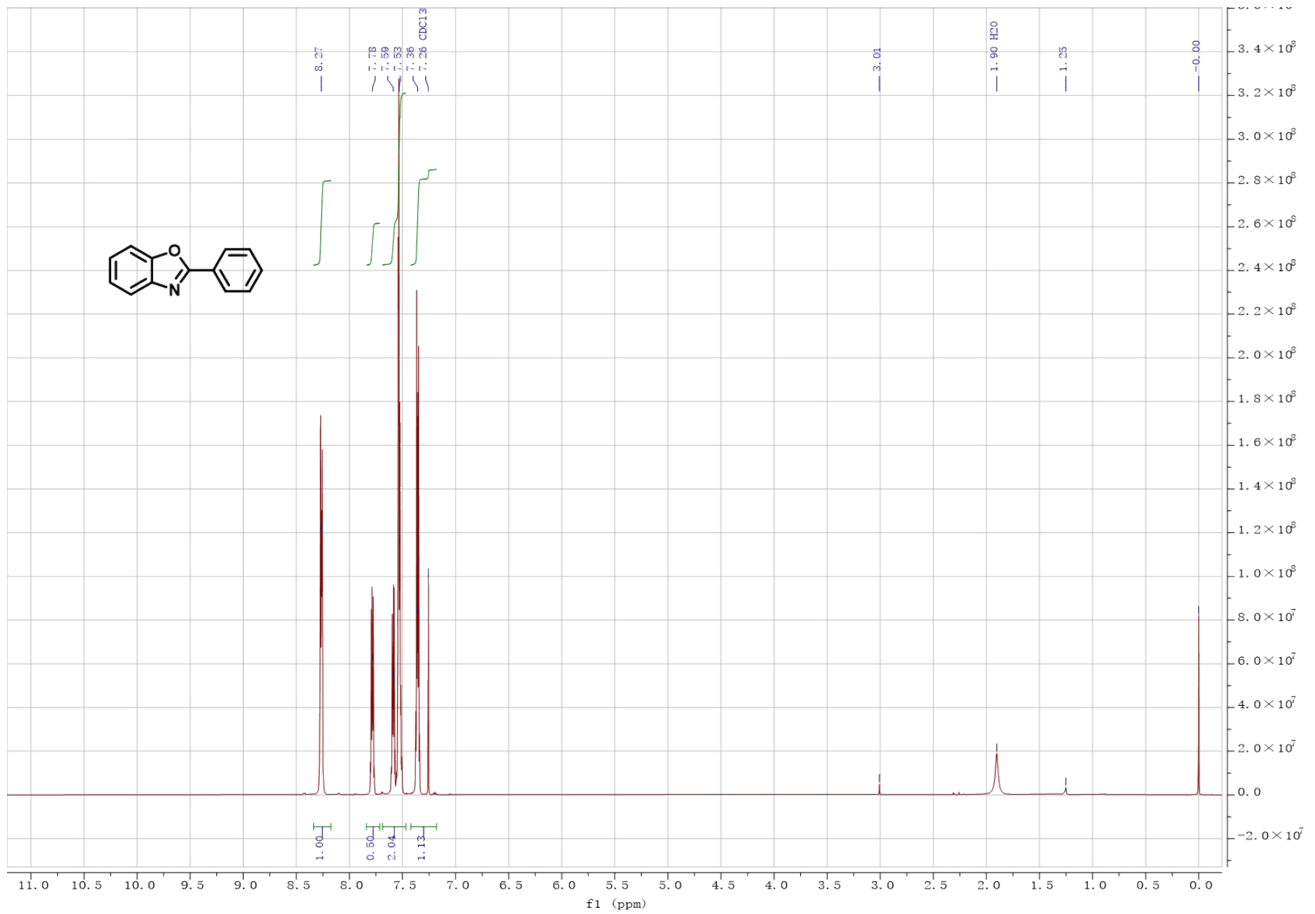
F7. 11. fid
13C NMR (126 MHz, CDCl₃) δ 140.81, 140.49, 125.75, 124.02, 119.82, 117.67.



F7. 12. fid
19F NMR (471 MHz, CDCl₃) δ -64.14.

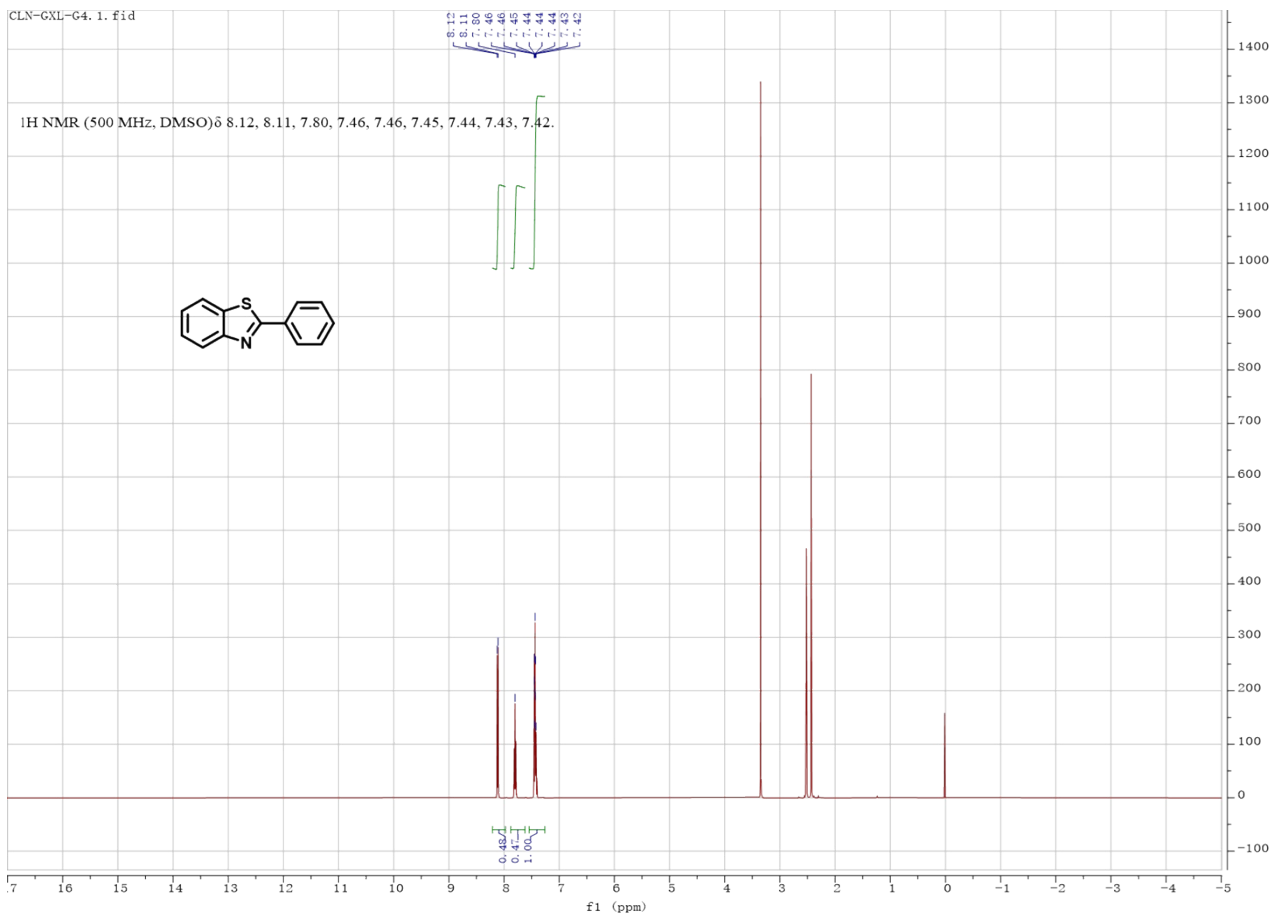
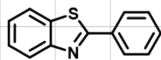






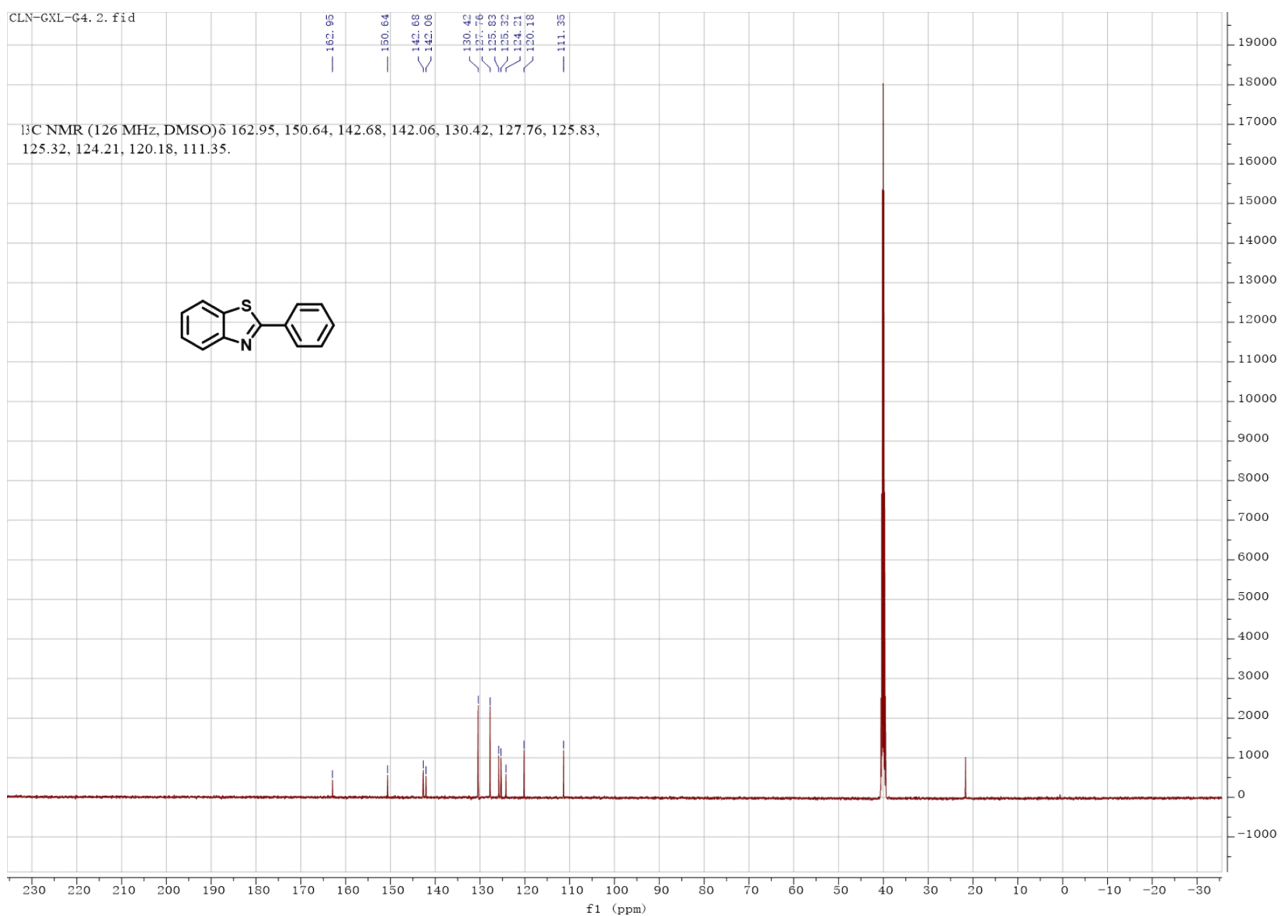
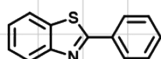
CLN-GXL-G4. 1. fid

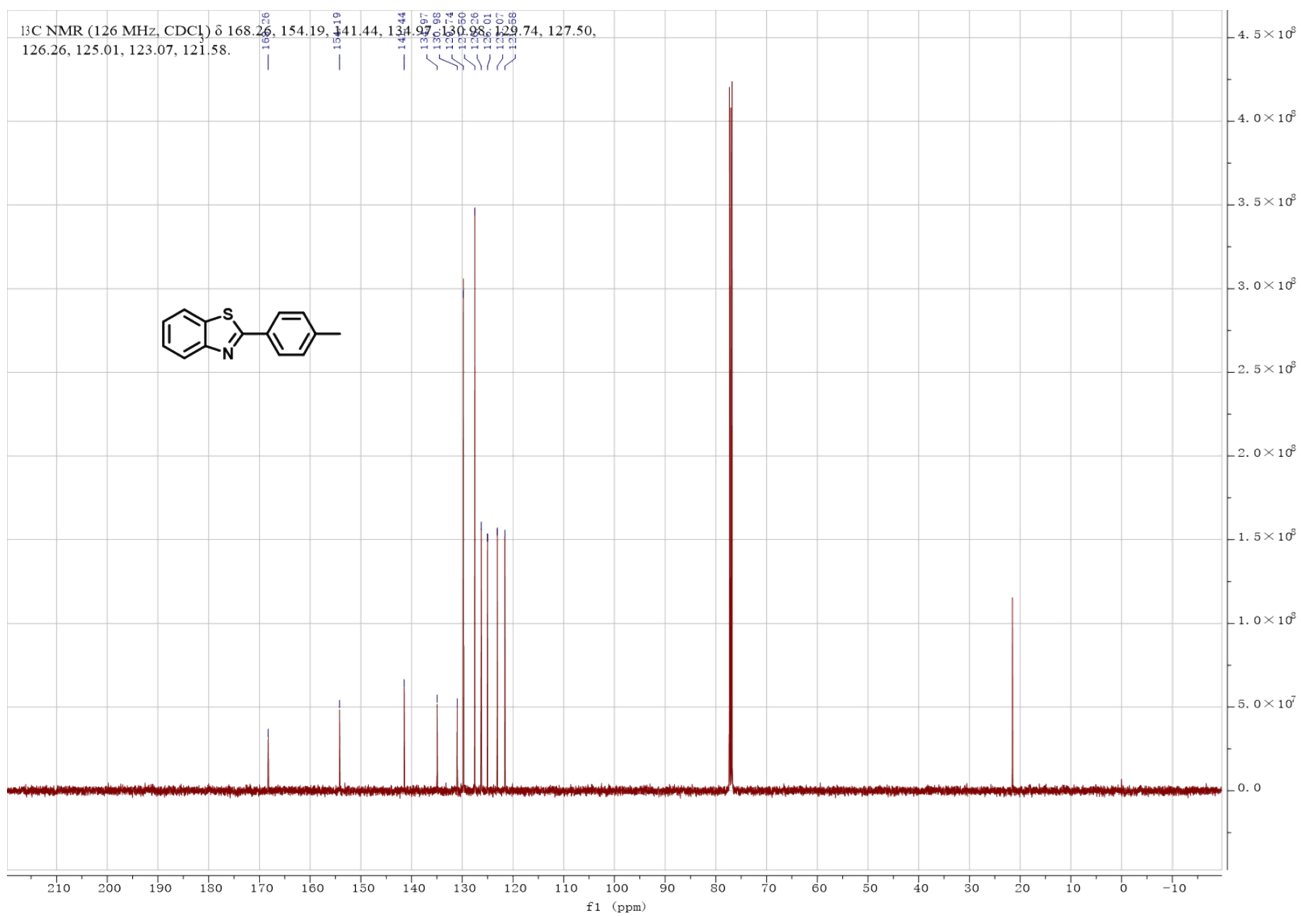
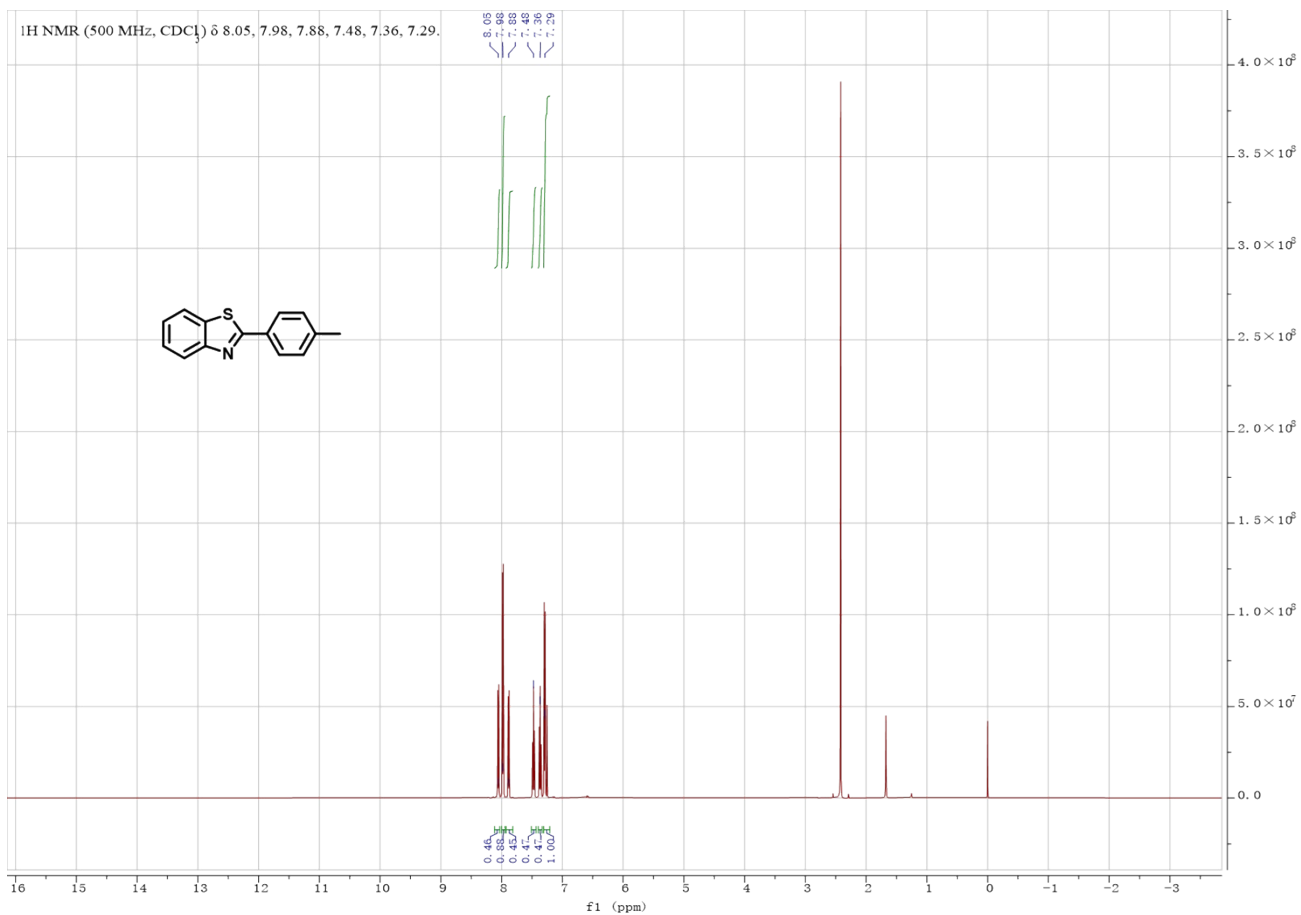
$^1\text{H NMR}$ (500 MHz, DMSO) δ 8.12, 8.11, 7.80, 7.46, 7.46, 7.45, 7.44, 7.43, 7.42.

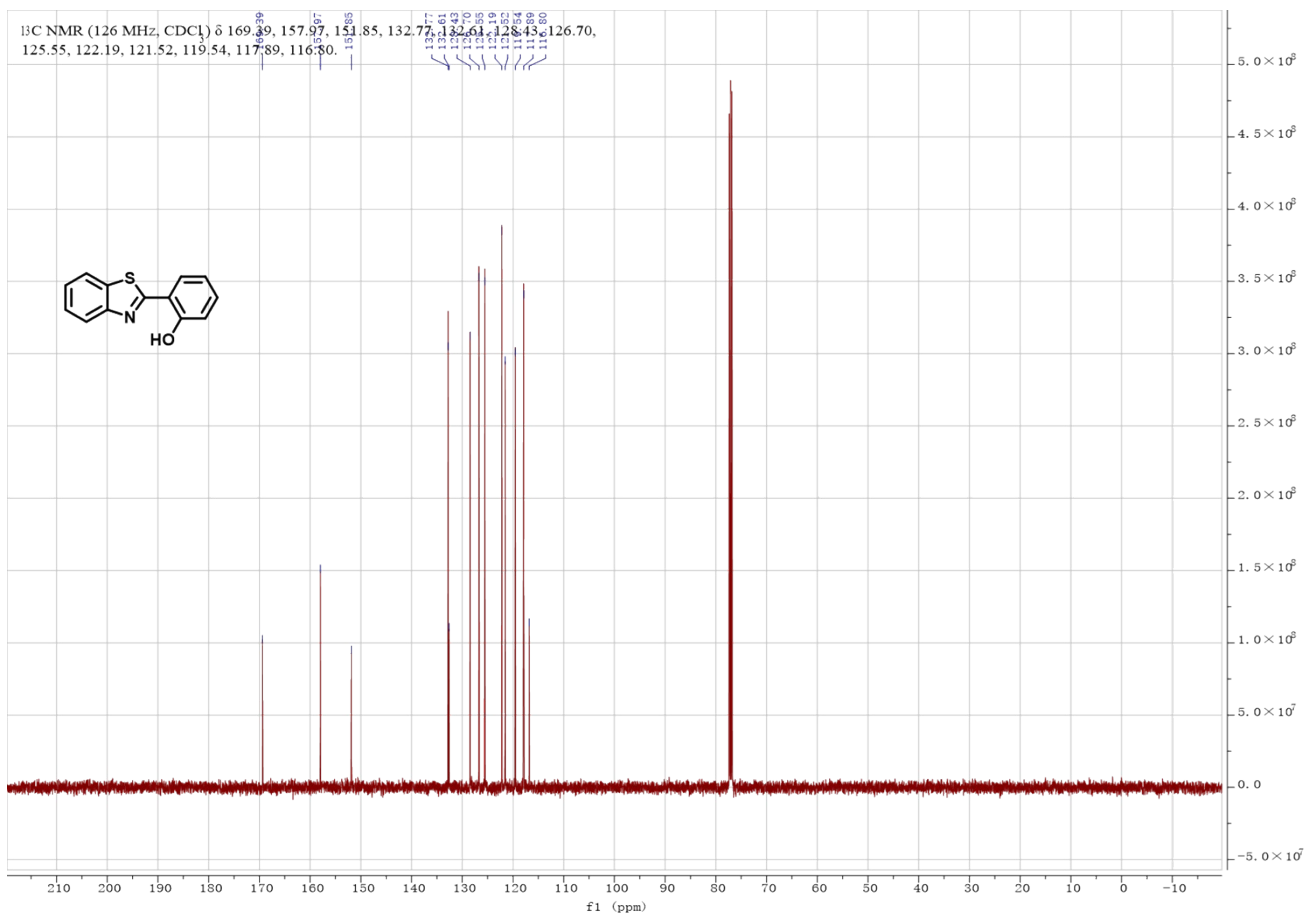
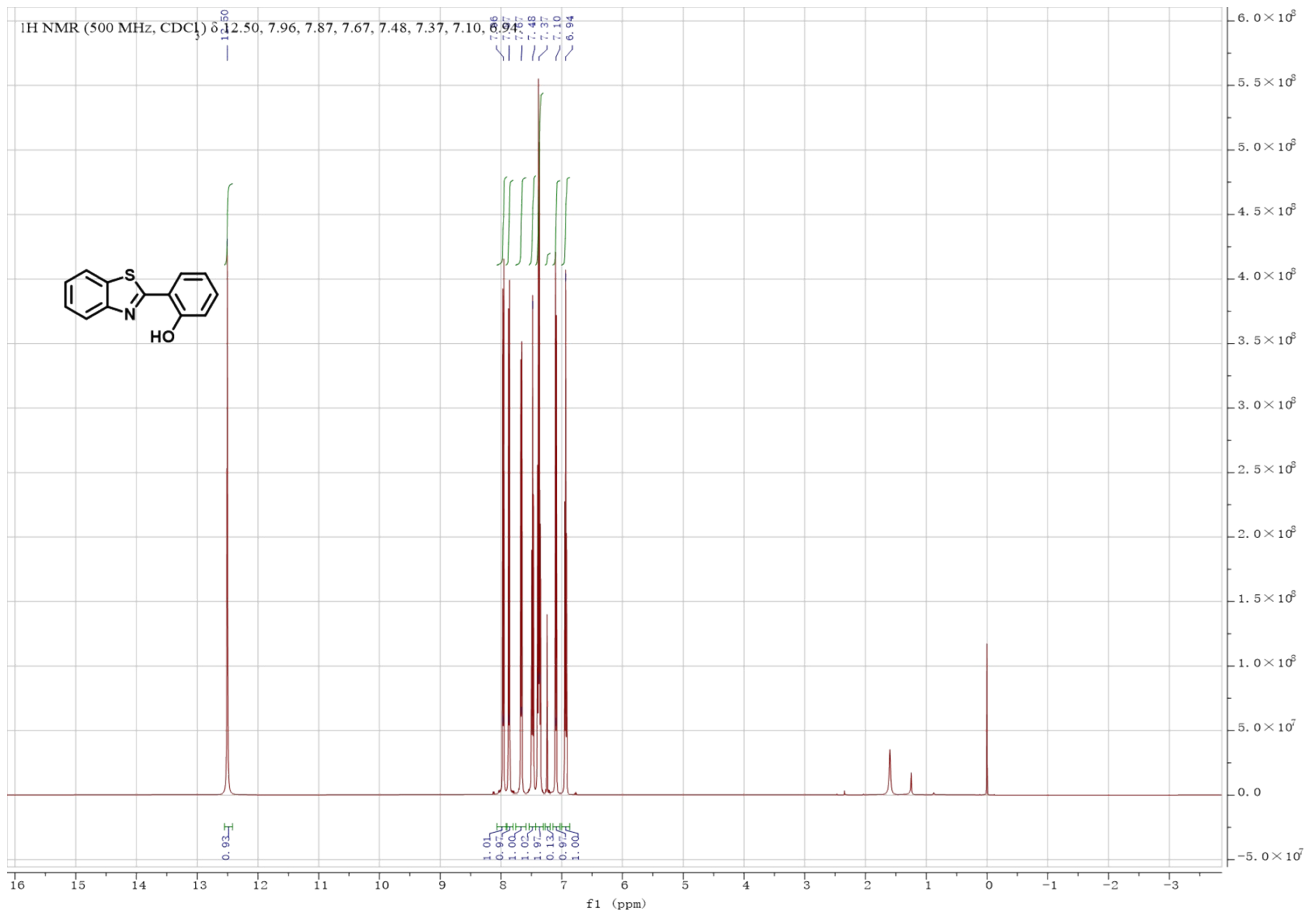


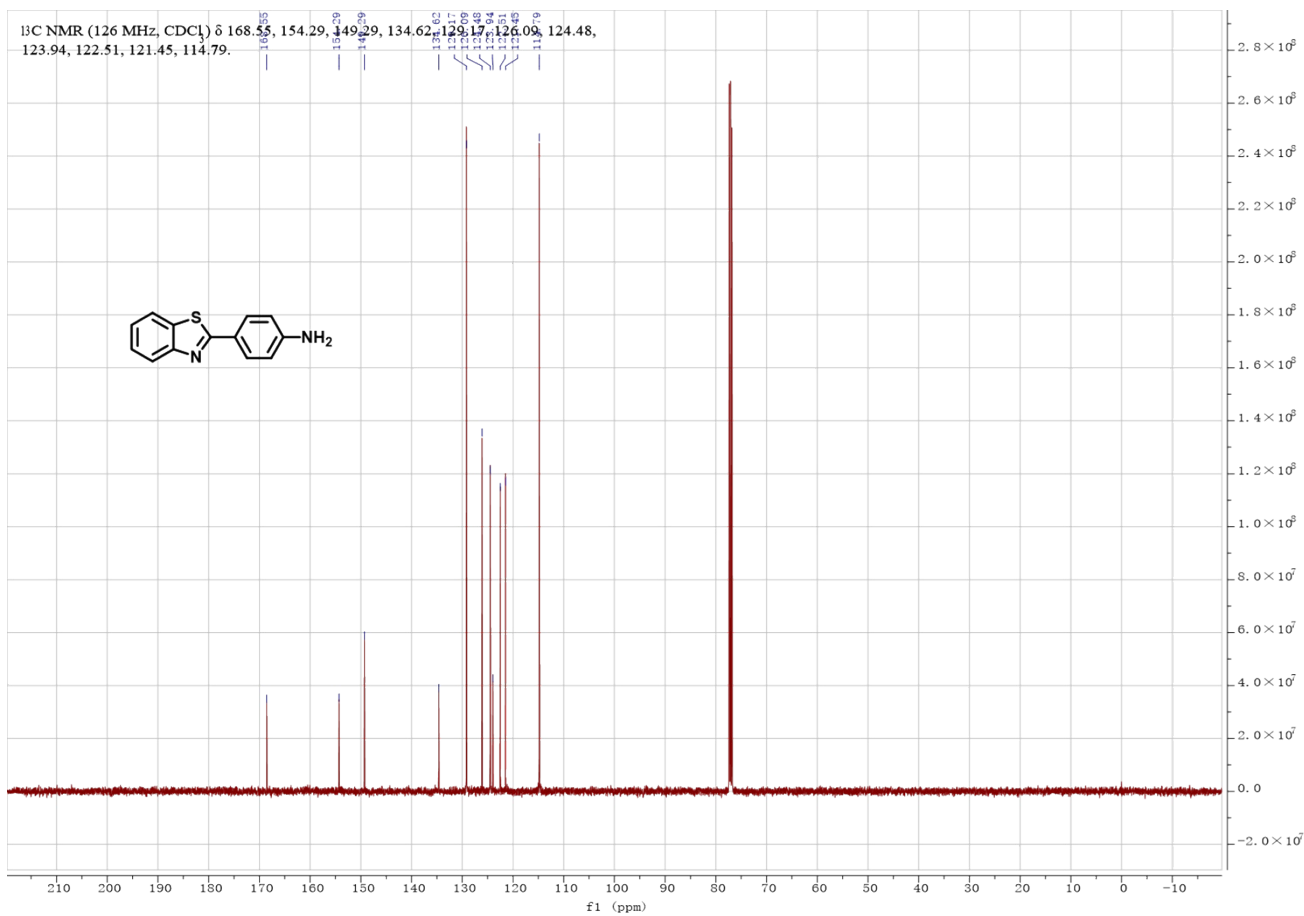
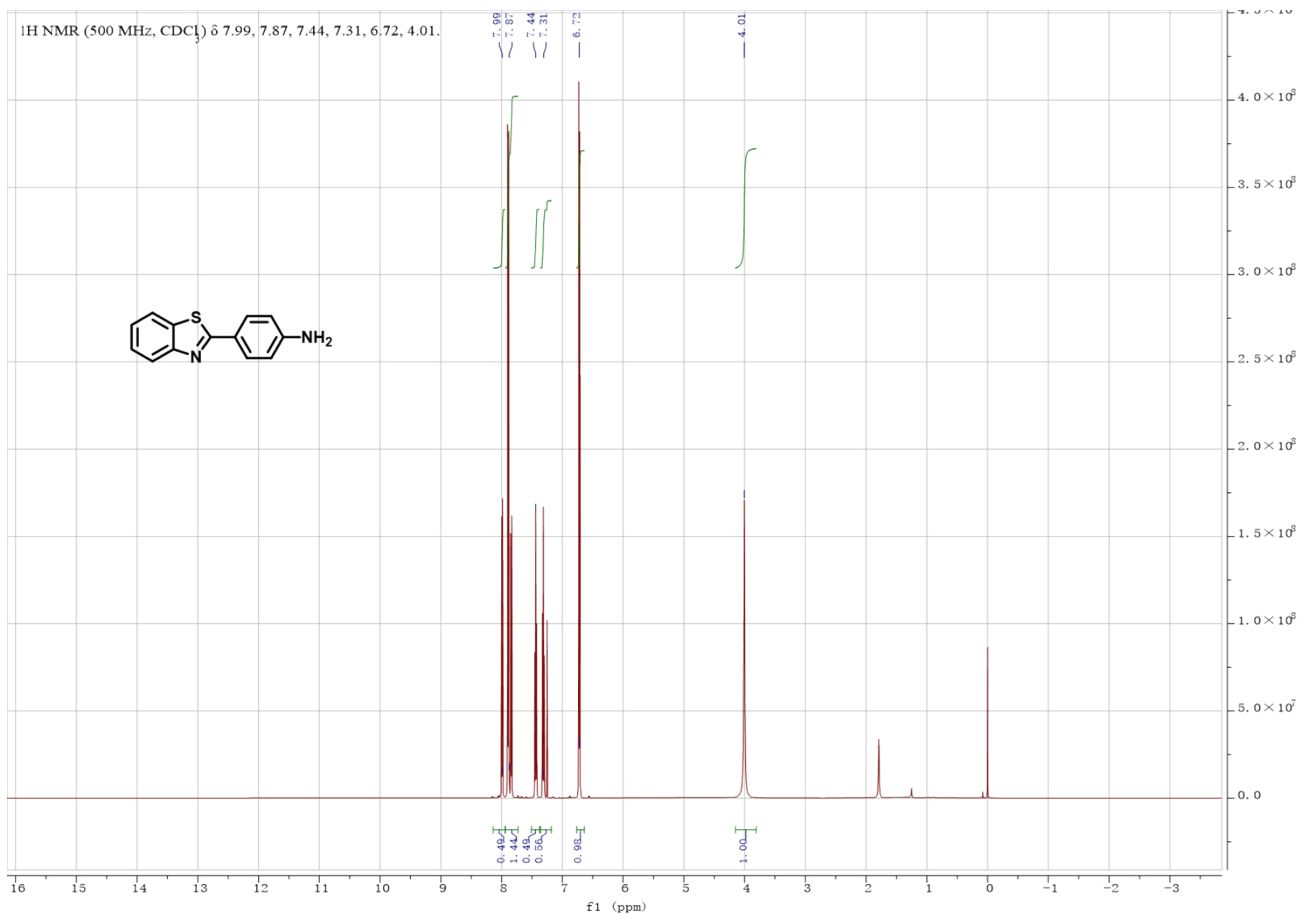
CLN-GXL-G4. 2. fid

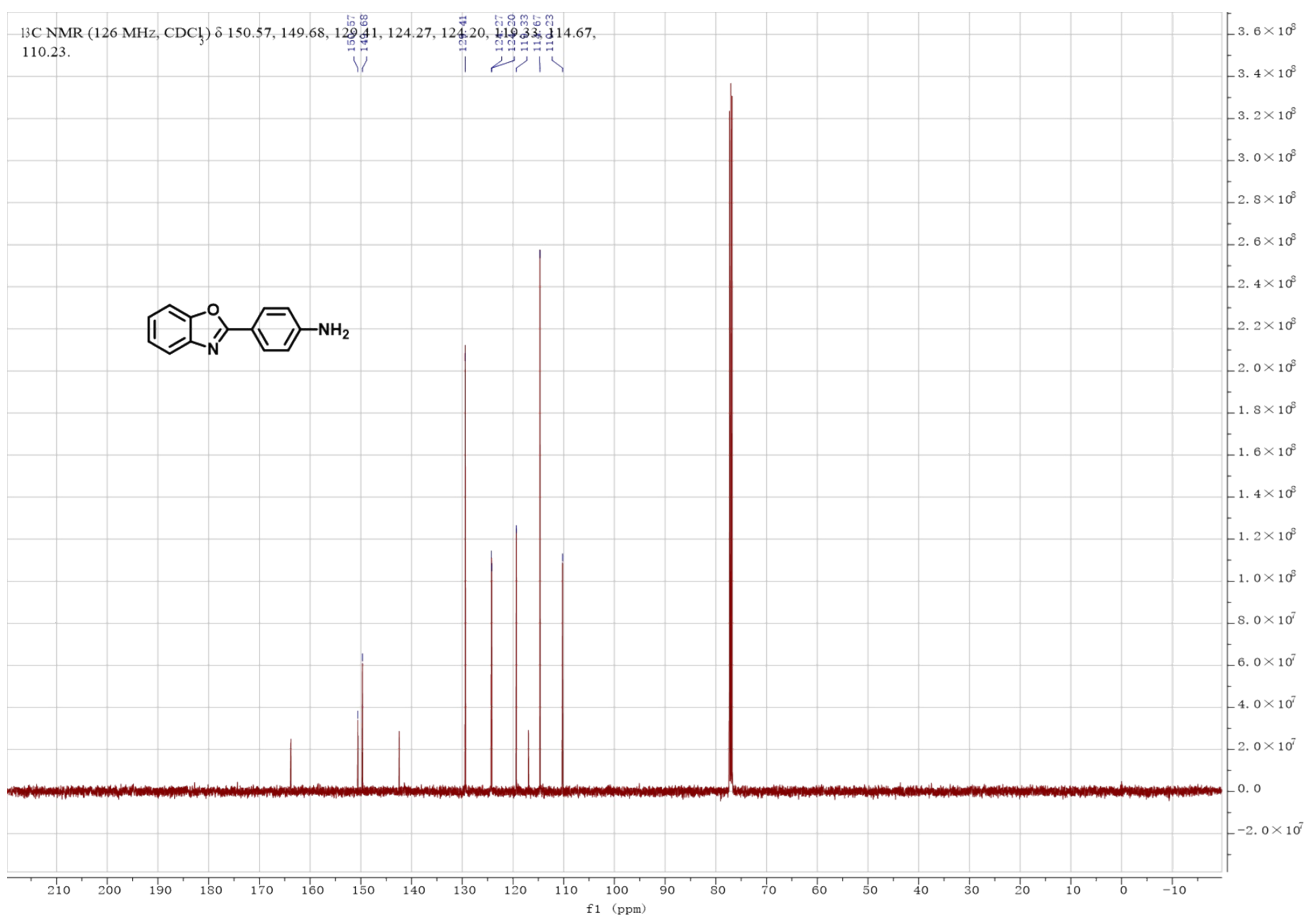
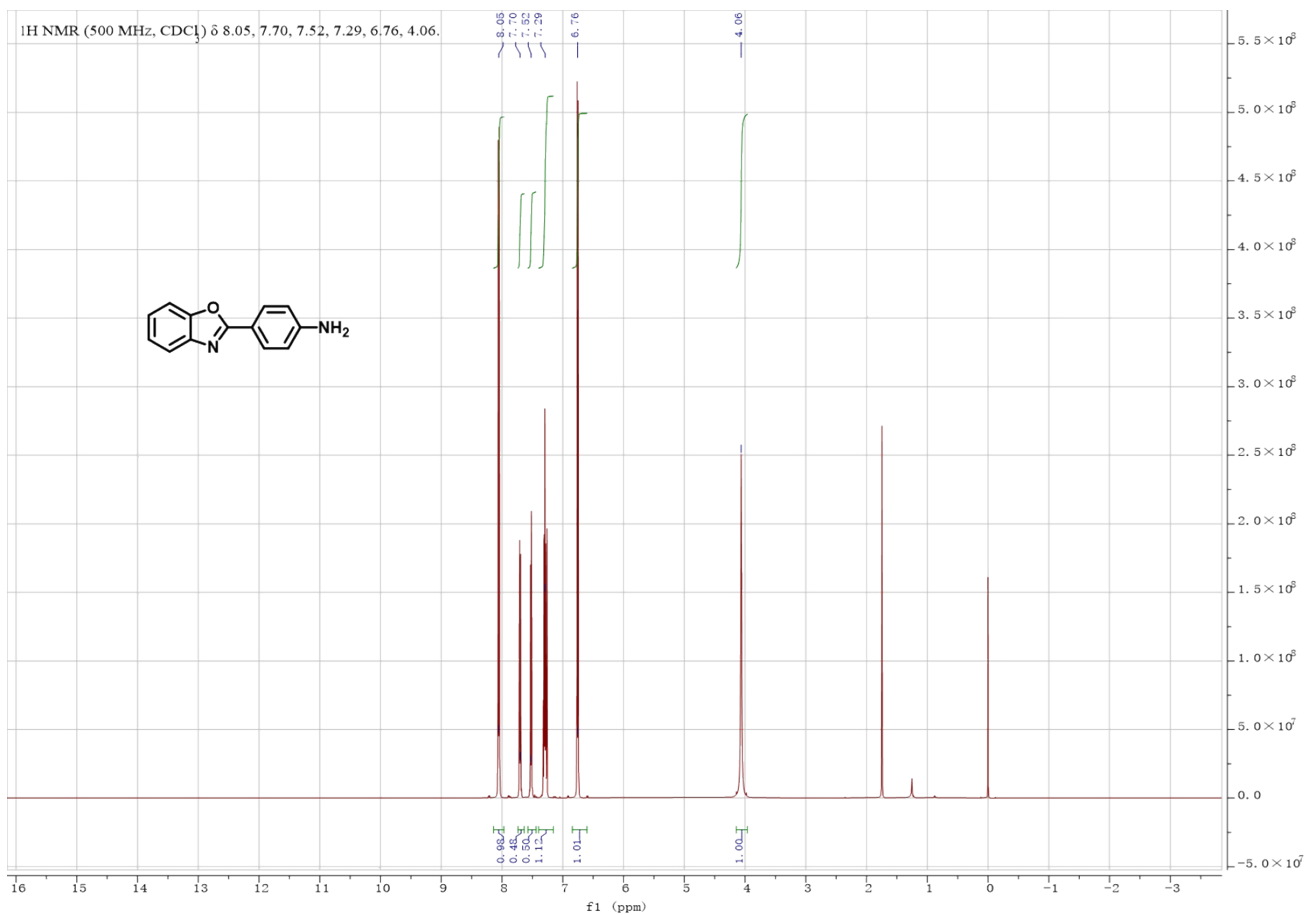
$^{13}\text{C NMR}$ (126 MHz, DMSO) δ 162.95, 150.64, 142.68, 142.06, 130.42, 127.76, 125.83, 125.32, 124.21, 120.18, 111.35.





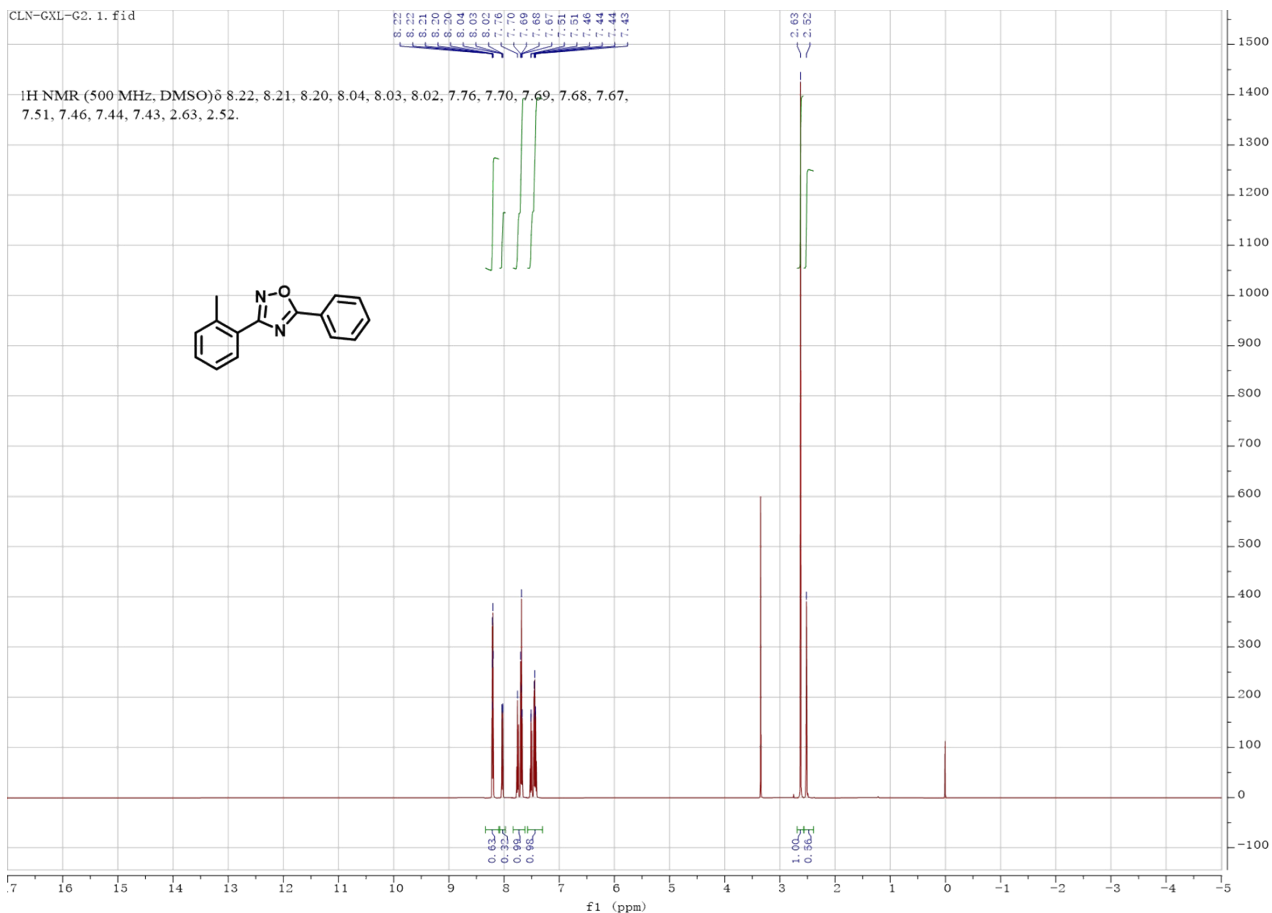
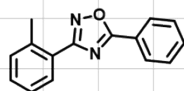






CLN-GXL-G2. 1. fid

¹H NMR (500 MHz, DMSO) δ 8.22, 8.21, 8.20, 8.04, 8.03, 8.02, 7.76, 7.70, 7.69, 7.68, 7.67, 7.51, 7.46, 7.44, 7.43, 2.63, 2.52.



CLN-GXL-G2. 2. fid

¹³C NMR (126 MHz, DMSO) δ 174.91, 169.41, 138.10, 133.81, 131.98, 131.47, 130.29, 130.09, 128.43, 126.77, 126.04, 123.91, 24.15, 22.11.

